UNIVERSITÀ DEGLI STUDI FIRENZE

DISEI DIPARTIMENTO DI SCIENZE PER L'ECONOMIA E L'IMPRESA

Working Papers - Economics

An interregional Input-Output model with spatiotemporal hydrological variability. The case of Tuscany

Gino Sturla and Benedetto Rocchi

Working Paper N. 26/2022

DISEI, Università degli Studi di Firenze
Via delle Pandette 9, 50127 Firenze (Italia) www.disei.unifi.it

Benedetto Rocchi[1]
Gino Sturla[2]

December 2022

Abstract

The work of Rocchi and Sturla (2021) presents an analysis of the pressure of the economic system on water resources in Tuscany at the regional level; in a following development Sturla and Rocchi (2022) incorporate temporal the hydrological variability to the regional model, with endogenous effects on agricultural and water for dilution demand. In this study, spatiotemporal variability is incorporated through i) a spatial disaggregation of the economic system based on an interregional input-output model (IRIO model) of Tuscan economy, ii) a spatial disaggregation of the hydrological components based on subregional data, and iii) a spatiotemporal model for the hydrological components based on a spatial stochastic model of precipitation. The spatial analysis scale corresponds to the Local Labor System (LLS), groups of contiguous municipalities classified based on economic criteria. Using the model developed, it is estimated the extended water exploitation index (EWEI), considering the extended demand (ED) and the feasible supply (FS) of water for each LLS; 100 hydrological years are simulated using a Montecarlo procedure. A novel endogenous scarcity threshold (ST) is proposed based on the results of the model and the intra-annual economic and hydrological characteristics of each LLS. With the EWEI and the ST, the hydro-economic equilibrium (HEE) for average hydrological conditions is characterised and the opportunity cost of the HEE is estimated. The latter corresponds to the minimum reduction of regional gross output compatible with the existence HEE in all LLS. Finally, the analysis is replicated considering a hydrology scenario under climate change.

Key Words: interregional input-output, hydrological variability, local economies, water stress, hydro-economic equilibrium, climate change.

JEL Classification: C67**,** Q25, Q50

The paper presents part of the results of the research project « IDROREGIO – A hydro-economic model for Tuscany » funded by the Italian Ministry of Environment within the National Strategy for Sustainable Development

[1] DISEI, Università degli Studi di Firenze. benedetto.rocchi@unifi.it
[2] DISEI, Università degli Studi di Firenze. ginostefano.sturlazerene@unifi.it

Contents

1 INTRODUCTION

The work of Rocchi and Sturla (2021) presents an analysis of the pressure of the economic system on water resources in Tuscany at the regional level. In a second paper later Sturla and Rocchi (2022) incorporate temporal hydrological variability to the regional model. This latest study shows that the value of the water exploitation index (EWEI) developed by Rocchi and Sturla (2021) does not exceed the critical threshold accepted in the literature and does not exceed the unit value (demand greater than supply) for the critical month in a 100 years simulation, considering both groundwater and surface water. However, this analysis assume spatial homogeneity of both water demand and supply (at the regional scale) and the perfect substitution between surface and groundwater. In fact, the EWEI for surface water far exceeds the thresholds used, which indicates that there may indeed be subregions with problems in the exploitation of their total resources (groundwater and surface water), given the heterogeneity in water supply and also in water demand.

The Tuscany region present an important spatial variability in terms of natural supply of water resources (Fatichi and Caporali, 2009; Bartolini et. al, 2018), and the uses of water (withdrawals and discharges) are quite heterogeneous (Venturi et al., 2014). In addition, the supply of water at a subregional scale does not necessarily fit with the resources required by production activities, whose location not necessarily is adapted to hydrological units and, mainly, due to the structure of surface water concessions within the river basins of the region (Venturi et al., 2014).

The above considerations indicate that the hydro-economic balance in Tuscany should be evaluated at a higher spatial resolution than the whole region. The main objective of this study is to build an inter-regional hydro-economic input-output model (with spatiotemporal hydrological variability) to study the relationship between the extended water demand (ED) and the feasible supply (FS) at subregional scale, estimating for each Local Labour System (LLS) the stochastic EWEI indicator.

We use the IRIO table of the Tuscany region containing 49 LLS, groups of contiguous municipalities classified according to an economic criterion (minimizing the flows of commuters who the boundaries across LLSs), and 53 industries. Multiregional input-output models (MRIO) have been widely used to study water use in economic systems, to quantify direct and indirect water consumed by industries in order to satisfy the final demand (Lenzen et al., 2013; Ridoutt et al., 2018; Velazquez, 2006) and for the estimation of virtual water flows and water footprint at regional, national and global scale (Feng et al., 2011, 2014; Duarte et al, 2016; Arto et al, 2016; White et al., 2015). These type of models have been recently used to estimate the water balance of economic systems, obtaining the water demand based on the economic model and determining the water supply based on water availability estimations. MRIO hydroeconomic models have been recently used to simulate demand shocks and their effect on the water balance (Cámara and Llop, 2020), and to sudy the impact of water supply constraints which affects production and the water balance in all regions of a MRIO model (Garcia-Hernandez and Brouwer, 2021).

Interregional input–output models have been implemented to study the interactions between the economy and the environment since the 1960's (Duarte and Yang, 2011). The interregional input–output table was developed based on the general regional (single-region) input–output table (Isard et al., 1960). With more information on transactions, it has been possible to implement interregional input-output models to assess environmental problems mainly linked to carbon emissions (Miller and Blair, 2009; Oosterhaven, 2014). The use of interregional input-output models considering water resources is frequent in the analysis of the water footprint (Zhuoying et al., 2011; Deng et al., 2016). The work of Zhuoying et al. (2001) assess the water footprint in the city of Beijing with an interregional model, considering only the blue water component. The main reason for ignoring green water is that in the short term it is relevant only in agriculture and the fact that it cannot be a substitute for water use by other sectors (Zhao, et al., 2010). The failure to consider grey water in the assessment of water footprint footprint is usually due to the lack of information and the complex nature of pollutants from different sectors (Zhuoying et al., 2011).

Most of the interregional models developed so far consider the province like the smaller economic unit of analysis, for the evaluation of the pressure of the economic system on the water resource. The model developed in this study considers a sub-provincial spatial scale, which allows a higher precision in the estimation of the hydro-economic balance. Moreover, to our knowledge until now, no interregional input-output model considers the spatiotemporal variability of the hydrological system, which is incorporated in this study.

Our approach does not correspond to water footprint analysis since what is of interest is the internal water used in production of each subregion. In this study, what is important are not the virtual flows of water (Guan and Hubacek, 2007), that is, the scope of the proposed model does not consist in determining the water contained in a product (e.g., considering the implicit water coming from imported inputs), but to estimate the amount of water extracted from each LLS for productive needs. The water used in production corresponds to surface and groundwater (blue water); part of the water used by agriculture comes from precipitation (green water) and is also considered the water required to dilute pollutants (grey water) .

As in the model developed at the regional scale by Sturla and Rocchi (2022), endogenous effects generated by hydrological variability are considered (at subregional scale), which correspond to: (i) variation in groundwater and surface water demand in agriculture, due to the lack of green water in years with dry hydrology (lower green water supply); and (ii) the change in water needs for dilution (grey water) in all discharging sectors, due to the dependence of pollutant concentration on surface runoff and groundwater recharge. In addition, in the case of water required for dilution, the effect of increased discharges from the agricultural sector due to losses associated with irrigation (second order endogenous effect) is added.

In this study we consider the precipitation availability as a proxy for green water availability (soil moisture) and evapotranspiration as a proxy for irrigation needs (Sturla and Rocchi, 2022), adapting estimates to the subregional scale. These two components allow us to incorporate variability into deterministic water use coefficients by industry and LLS, generating an endogenous effect, i.e., the extended demand of the agricultural sector changes according the hydrological components of each hydrological year and each LLS, also affecting the EWEI indicator.

To calculate the dilution requirements (grey water) we consider the reformulated mixing model developed by Rocchi and Sturla (2022), based on the Guan and Hubacek (2008) and Xie (1996) approach and the extended version of Rocchi and Sturla (2021). This mixing model considers the variability of pollutants concentration in fresh water bodies (due to changes in groundwater recharge and surface runoff), where a portion is reserved for dilution purposes (as a share of the extended demand for water). The chemical oxygen demand COD is considered as an indicator of the water quality, since it corresponds to an important indicator of water quality in industrial sectors (Meng et al., 2018; Wang et al., 2022).

Regarding water scarcity indicators, Cámara and Llop (2020) use the input-output model to study the sustainability of water use in the region of Catalonia (Spain), by estimating the water exploitation index (WEI^{+}) (European Environmental Agency, 2005; Faergemann, 2012; OECD, 2015). A threshold value of 20% for the WEI is used as a sustainability criterion. This threshold has been recommended and used to define water stress, as well as a value of 40% has been proposed to differentiate moderate and severe shortages, considering very general elements on regulation capacity and extraction feasibility (Raskin et al., 1997; Alamo et. al, 2000, Pfister et al., 2009, CIRCABC, 2012). However, the threshold for water scarcity does not consider explicitly the intra-annual variability of water demand and supply. Another recent important contribution is the study of Garcia-Hernandez and Brouwer (2021), which develops a water-restricted MRIO model to evaluate the direct and indirect impacts of possible future water use restrictions due to climate change on economic activities around the Great Lakes region. The water availability index (WAI), defined as the ratio of water withdrawals to renewable water availability (OECD, 2015; Pfister et al., 2009), is used as an indicator of water balance. The work considers the standard threshold values, 20% for scarcity and 40% for severe scarcity.

Aiming to incorporate local characteristics (economic as well as hydrological) into the scarcity assessment, we propose a novel scarcity threshold (STg) for the EWEI which is defined as the minimum value of the annual EWEI ensuring that ED does not exceed the FS in any month. The STg varies according to the characteristics of each subregion, taking into account both hydrological and economic intra annual variability. STg also considers natural groundwater regulation capacity (optimal intra-annual groundwater management). The STg is endogenous in the model, i.e. changes in the economic production generate a modification of this threshold. Moreover, due to inter-regional and inter-industry links, a change in demand in one sector of a subregion could generates a change in the ST of the other subregions. This allows a deeper understanding of water scarcity in the hydro-economic system.

Based on the extended water exploitation index (EWEI) obtained from the hydro-economic IRIO model and the endogenous scarcity threshold (STg) proposed in this study, we define the local hydro-economic equilibrium (LHEE) as the situation in which the EWEI does not exceed STg in a given subregion; and regional hydro-economic equilibrium (RHEE) when STg is not exceeded in any subregion in the average hydrology scenario. When some subregions the LHEE is missed, we define the opportunity cost of RHEE as the minimum reduction of the regional production, compatible with the achievement of the LHEE in all sub-regions. That is, water availability constraints are incorporated into the economic IRIO model, an approach that has been scarcely present in literature (Garcia-Hernandez and Brouwer, 2021).

Regarding the hydrological model with spatiotemporal variability, first of all a disaggregation of the components of the regional average hydrology is carried out: precipitation, evapotranspiration, groundwater recharge and surface runoff (Sturla and Rocchi, 2022). This disaggregation considers the precipitation map of the region, the agricultural area, and the spatial pattern of groundwater and surface water concessions. The disaggregation methodology maintanins the coherence between these components at the river basin level, despite the unit of analysis (LLS) does not correspond to a hydrological unit, showing as a consequence imbalances between the hydrological components.

For the incorporation of temporal variability, a spatial stochastic model for precipitation is considered, based on meteorological information from 42 precipitation stations distributed in the region. This methodology considers a smoothing of the spatial correlation matrix due to missing data at some stations. The model allows to generate annual precipitation series for each LLS with a spatial correlation structure. Based on the results of the spatial disaggregation of the mean hydrology, the spatiotemporal variability of evapotranspiration, groundwater recharge and surface runoff is incorporated, evaluating the coherence of the model based on its aggregation at the regional level and the comparison with the statistics of the regional series of the hydrological components.

Chapter 2 of this study presents the regional hydrology de-aggregation methodology and the stochastic hydrologic model for the incorporation of spatial-temporal variability. Chapter 3 develops the methodology of the IRIO hydro-economic model, considering the adaptation of the Sturla and Rocchi (2022) model to a subregional context and adding the methodology for determining the endogenous scarcity threshold, the definition of the hydro-economic equilibrium and its opportunity cost. In addition, this chapter describes the disaggregation of water use coefficients at the subreginal scale. Chapter 4 presents the main results of the study, studying the hydro-economic balance at the subregional level based on the EWEI and STg indicators, determining for each LLS how many times the threshold is exceeded in 100 years and estimating the regional opportunity cost of the hydro-economic balance for an average hydrological conditions; the analysis is replicated for hydrological scenario with climate change. Finally, Chapter 5 summarize and discusses the results.

2 MODELLING SUBREGIONAL HYDROLOGY

2.1 Average subregional hydrology

A spatial disaggregation is carried out for each of the variables of the hydrological cycle: i) for precipitation, the regional total has been disaggregated based on the precipitation map of Tuscany; ii) for evapotranspiration, it is considered the agricultural area and the precipitation in each LLS; iii) for the groundwater recharge, it is considered the maximum water volume of concessions and the estimated precipitation; and iv) for runoff, it is considered the corrected volume of concessions and the precipitation. The period considered correspond to 1970-2010 as well as the study of Sturla and Rocchi (2022). In this paper, LLS have also been referred to as sub-regions.

2.1.1 Precipitation

Subregional precipitation is calculated based on the precipitation map of the region (SIR, 2021), using GIS tools. The precipitation map was constructed for the period 1994-2014. The average precipitation value for the region corresponds to 1,023 mm per unit of area. Since the regional precipitation value for the period 1971-2010 equal to 882 mm per unit of area (20,269 Mm^3) (Rocchi and Sturla, 2021; ISTAT, 2021), a correction is made to obtain an average precipitation ($\bar{P}^s$ in Mm^3) in each subregion *s*, representative of the study period.

$$\bar{P}^s = \frac{p^s_{94/14} \cdot A^s_T}{1000} \cdot \frac{p^{Reg}_{71/10}}{p^{Reg}_{94/14}} \tag{2.1}$$

where,

$p^s_{94/14}$	:	Precipitation in subregion s, period 1994-2014 (mm)
A^s_T	:	Total area of subregion s (km^2)
$p^{Reg}_{71/10}$	:	Mean regional precipitation, period 1971-2010 (mm)
$p^{Reg}_{94/14}$	:	Mean regional precipitation, period 1994-2014 (mm)

The mean value of precipitation volumes for the LLS corresponds to 414 Mm^3, the standard deviation is 275 Mm^3 and the coefficient of variation is 66%.

Figure 2-1 shows the precipitation map for the whole region. Figure 2-2 present the estimated precipitation by LLS.

Figure 2-1. Precipitation map for Tuscany (1994-2014)

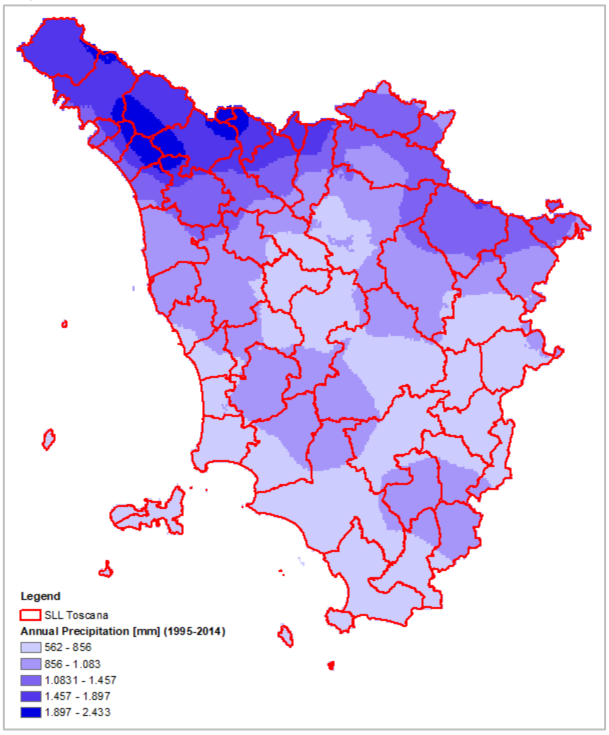

Source: own elaboration based on SIR (2021)

Figure 2-2. Precipitation by LLS (average value, 1970-2010)

Precipitation (mm) | Precipitation (Mm3)

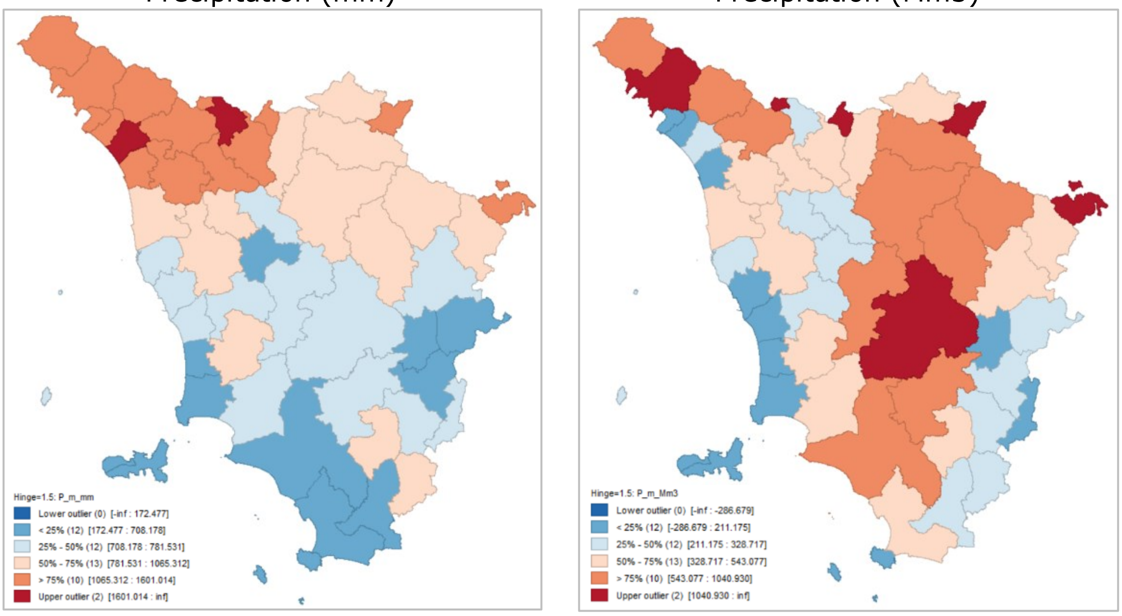

Source: own elaboration

2.1.2 Evapotranspiration

For the estimation of subregional evapotranspiration, a methodology of disaggregation of the regional evapotranspiration estimated by Rocchi and Sturla (2021), equal to 11,890 Mm^3 (557 mm per unit of area), is proposed.

The evapotranspiration of each LLS is estimated as a linear combination of the ratio of agricultural to the regional agricultural area and the ratio of the precipitation to regional precipitation.

The agricultural area accounts for only a part of the evapotranspiration, however, as evapotranspiration depends also on transpiration from non-agricultural plant areas and evaporation from soil and other sources. Since total evapotranspiration is conditioned by available water (precipitation), this variable is included for disaggregation purposes.

The percentage of agricultural area has the function of adding heterogeneity to the evapotranspiration disaggregation, which will be more intense the more agriculture is involved.

Let $\bar{E}^s$ be the mean evapotranspiration for subregion s, then:

$$\bar{E}^s = \left[\tau \frac{A_A^s}{A_A^{Reg}} + (1-\tau)\frac{\bar{P}^s}{\bar{P}^{Reg}}\right] \cdot \bar{E}^{Reg} \tag{2.2}$$

where,

A_A^s	:	Agricultural area of subregion s (km^2)
A_A^{Reg}	:	Agricultural area of the region (km^2)
$\bar{P}^s$	:	Precipitation of subregion s (Mm^3)
$\bar{P}^{Reg}$	:	Precipitation of the whole region (Mm^3)
$\bar{E}^{Reg}$	:	Mean evapotranspiration of the region (Mm^3)
τ	:	Weight of total area ratio in the estimate $\tau \in (0,1)$

The estimation assumes a value of $\tau = 0.4$, i.e., it is assumed that 40% of the evapotranspiration depends on the agricultural area and 60% on the water available for evapotranspiration.

Information on agricultural area at subregional scale is obtained from ISTAT (2021). It represents 36% of the total area of the region (8,345 km^2 and 22986 km^2).

Figure 2-3 shows the average evapotranspiration estimated by LLS in volume and as a percentage of the average precipitation of each LLS.

The mean value of evapotranspiration volume for the subregions corresponds to 243 Mm^3, the standard deviation is 163 Mm^3 and the coefficient of variation is 67%. Evapotranspiration represents 61% of precipitation on average, with a maximum value of 88% and a minimum value of 37%.

Figure 2-3. Evapotranspiration by LLS (average value, 1970-2010)

Evapotranspiration (Mm^3) | Evapotranspiration (% of P)

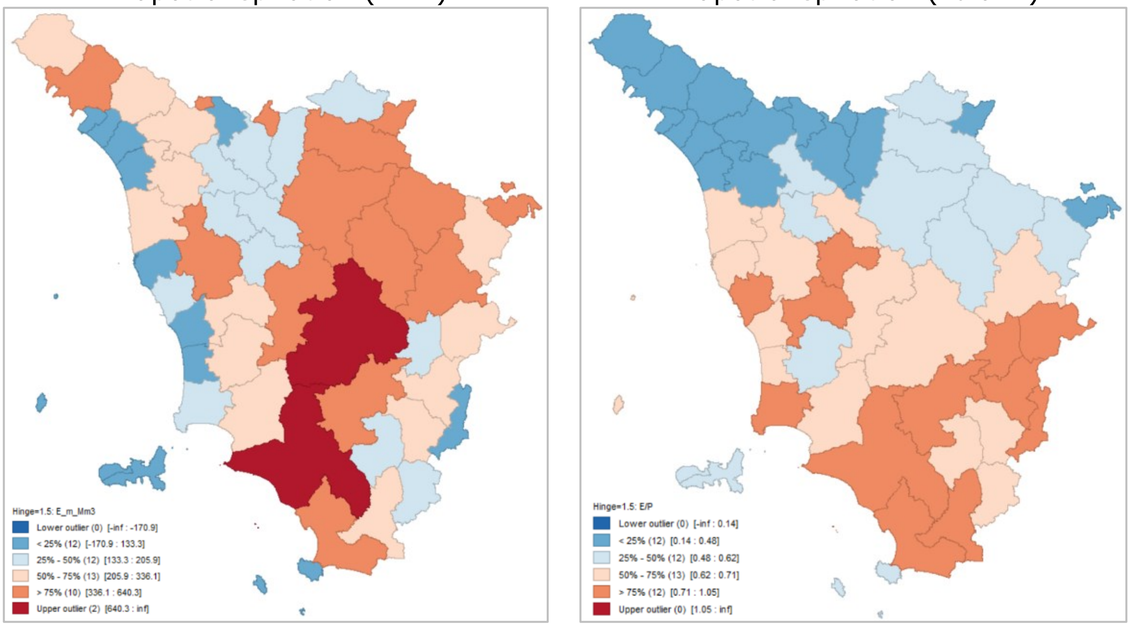

Source: own elaboration

2.1.3 Groundwater recharge

The regional groundwater recharge corresponds to 4,155 Mm^3 (Rocchi and Sturla, 2021), which is disaggregated at the LLS level considering the available information on volume of water concessions contained in two databases (SIR, 2021; Distretto Appenino Settentrionale, 2021). For each identified extraction point, the maximum value between the two databases is considered.

The concessions fit fairly well with the identified aquifers (Figure 2-X). However, since the total value known of the concessions is less than the total regional recharge (2,699 Mm^3, 65% of the regional value), and they may not be fully representative of the actual water that can be sustainably extracted, a disaggregation methodology based on the ratio of the volume of concessions to the regional total and the precipitation of each subregion to the regional precipitation is assumed. The average groundwater recharge by subregion ($\bar{I}^s$) is estimated as:

$$\bar{I}^s = \left[\varphi \cdot \frac{max(G_C^s, G_W^s)}{\sum_s max(G_C^s, G_W^s)} + (1-\varphi) \cdot \frac{\bar{P}^s}{\bar{P}^{Reg}}\right] \cdot \bar{I}^{Reg} \qquad (2.3)$$

where,

G_C^s	:	Groundwater concessions volume database SIR (2021) (Mm^3)
G_W^s	:	Groundwater concessions volume database Distretto (2021) (Mm^3)
$\bar{P}^s$	:	Average precipitation of subregion s (Mm^3)
$\bar{P}^{Reg}$	:	Regional average precipitation (Mm^3)

$\bar{I}^{Reg}$: Regional average groundwater recharge (Mm^3)

φ : Weight of concessions $\varphi \in (0,1)$

The estimation assumes a value of $\varphi = 0.5$, i.e., it is assumed that 50% of the groundwater recharge depends on groundwater concessions and 50% on the water available for recharge.

The mean value of groundwater recharge volume for the subregions corresponds to 85 Mm^3, the standard deviation is 102 Mm^3 and the coefficient of variation is 120%. Groundwater recharge represents 21% of precipitation on average, with a maximum value of 155% and a minimum value of 10%.

Figure 2-4 presents the aquifers and the concession points. Figure 2-5 show the groundwater recharge estimated by LLS (volume and percentage of precipitation).

Figure 2-4. Aquifers and groundwater concessions

Aquifers area | Concessions

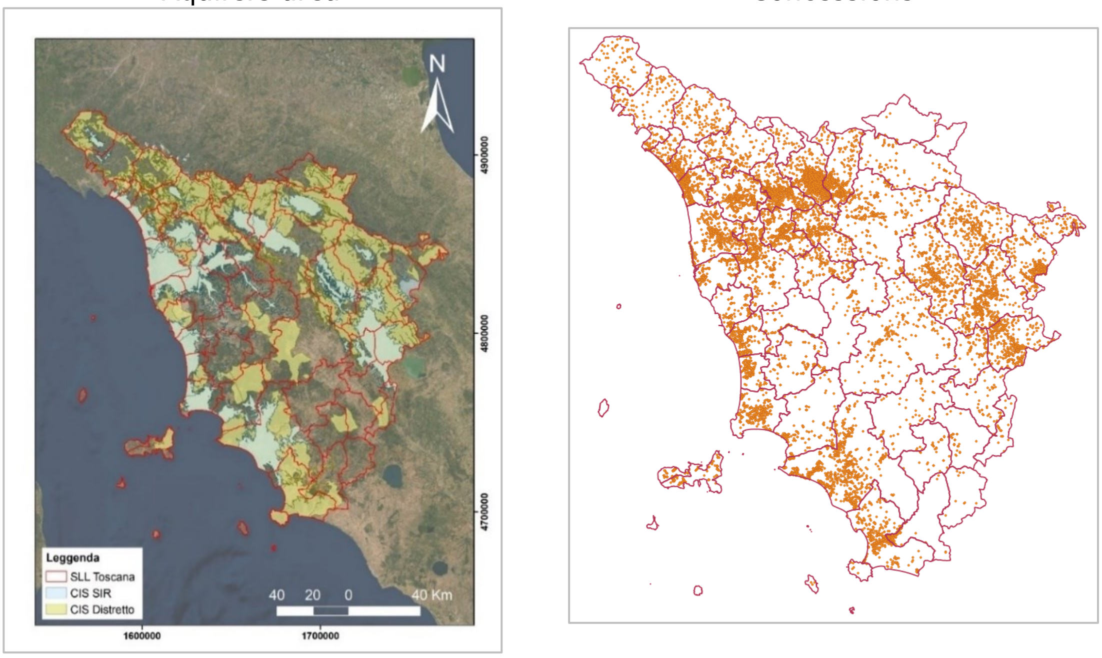

Source: own elaboration based on SIR (2021) and Distretto Appenino Settentrionale (2021)

Figure 2-5. Groundwater recharge by LLS

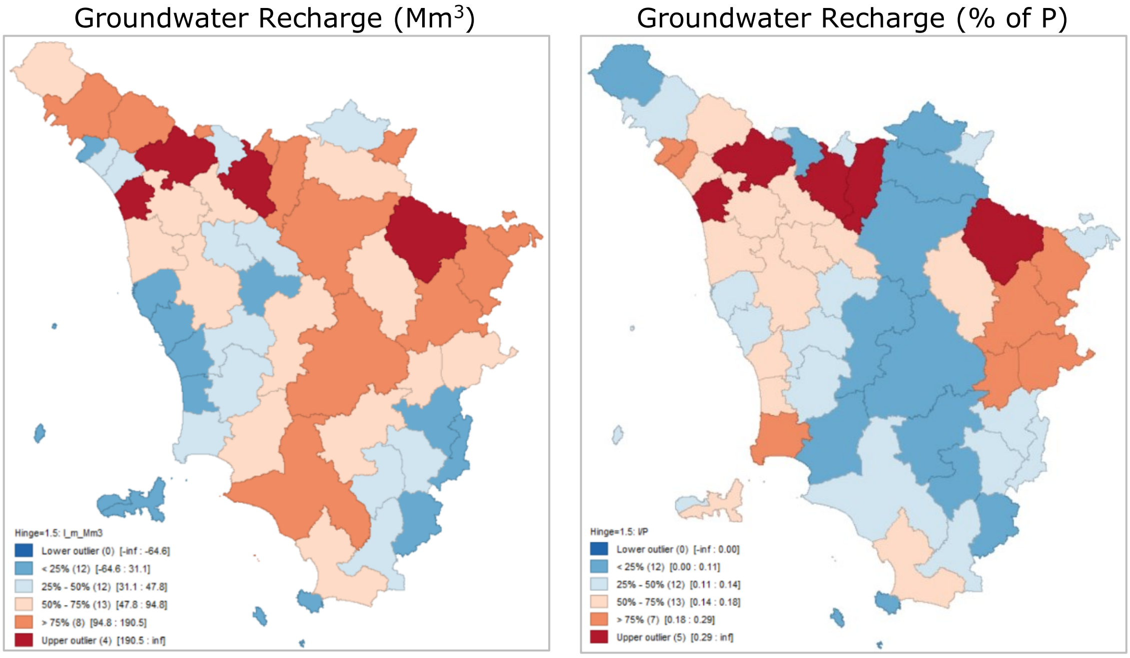

Source: own elaboration

2.1.4 Surface runoff

Determining the surface runoff associated with each subregion is a complex task because, on the one hand, they do not correspond to hydrological units and, on the other hand, it is possible that water generated in upstream LLSs is actually available for a downstream LLS. For this reason, the volumes of surface water concessions granted and the precipitation (both with respect to the regional total) of each subregion are considered.

Based on information from the SIR (2021) the sum of surface water concessions for consumptive uses in the region corresponds to 1,959 Mm^3. However, this information corresponds to 70% of the concessions for the entire region (Venturi et al., 2014), i.e. the total volume of concessions corresponds to 2,605 Mm^3, 68.5% of the regional runoff of 3,803 Mm^3 (Rocchi and Sturla, 2021). Figure 2-6 shows the surface water concessions.

The lack of information is not homogeneous across the region. The smallest spatial scale with information on the incompleteness of the concession register corresponds to the province. Venturi et al. (2014) present this information, according to Table 2-1.

Table 2-1. Missing concessions volume by province

Province	Missing concessions volume
Arezzo	25%
Firenze	5%
Grosseto	80%
Livorno	65%

Province	Missing concessions volume
Lucca	5%
Massa-Carrara	15%
Pisa	45%
Pistoia	20%
Prato	25%
Siena	65%

Source: Venturi et al. (2014)

Figure 2-6. Surface water concessions

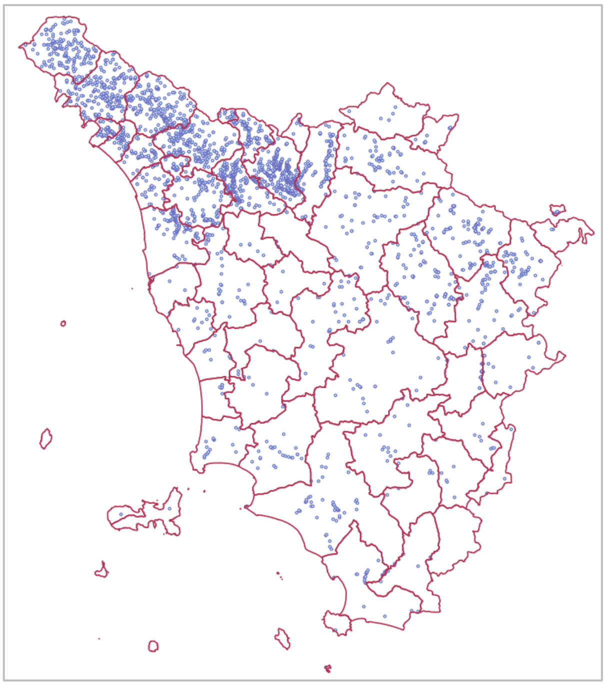

Source: own elaboration based on SIR (2021)

For the determination of the total surface concessions per LLS, a methodology is proposed that distributes the missing volume in each province among the LLS's that compose it. This methodology assumes a relationship of proportionality between concessions and water withdrawals, for the average condition (water withdrawals calculated on the basis of the IRIO model). Thus, corrected surface water concessions volume ($\tilde{C}^s$) is written as:

$$\tilde{C}^s = C^s + C^p \frac{W^s}{W^p} \frac{\lambda^p}{1 - \lambda^p} \tag{2.4}$$

where,

C^s	:	Surface water concessions volume in subregion s (Mm^3)
C^p	:	Surface water concessions volume in province p (Mm^3)
W^s	:	Surface water average withdrawals volume in subregion s (Mm^3)
W^p	:	Surface water average withdrawals volume in province p (Mm^3)
λ^p	:	Percentage of missing concessions volume in province p

The mean surface runoff for subregion s ($\bar{R}^s$) is estimated as a linear combination of the proportion of concessions and precipitation.

$$\bar{R}^s = \left[\xi \cdot \frac{\tilde{C}^s}{\sum_s \tilde{C}^s} + (1-\xi) \cdot \frac{\bar{P}^s}{\bar{P}^{Reg}}\right] \cdot \bar{R}^{Reg} \tag{2.5}$$

Where $\bar{R}^{Reg}$ corresponds to the regional average runoff. We assume a weigh $\xi = 0.3$ for the concessions. This factor generates consistency at the basin level (section 2.1.5), which is important, since there may be water transfers between LLSs but not between basins that are not hydraulically connected.

The mean value of surface runoff volume for the subregions corresponds to 78 Mm^3, the standard deviation is 79 Mm^3 and the coefficient of variation is 102%. Groundwater recharge represents 19% of precipitation on average, with a maximum value of 85% and a minimum value of 13%.

Figure 2-7 show the surface runoff estimated by LLS (volume and percentage of precipitation).

Figure 2-7. Surface Runoff by LLS (average, 1970-2010)

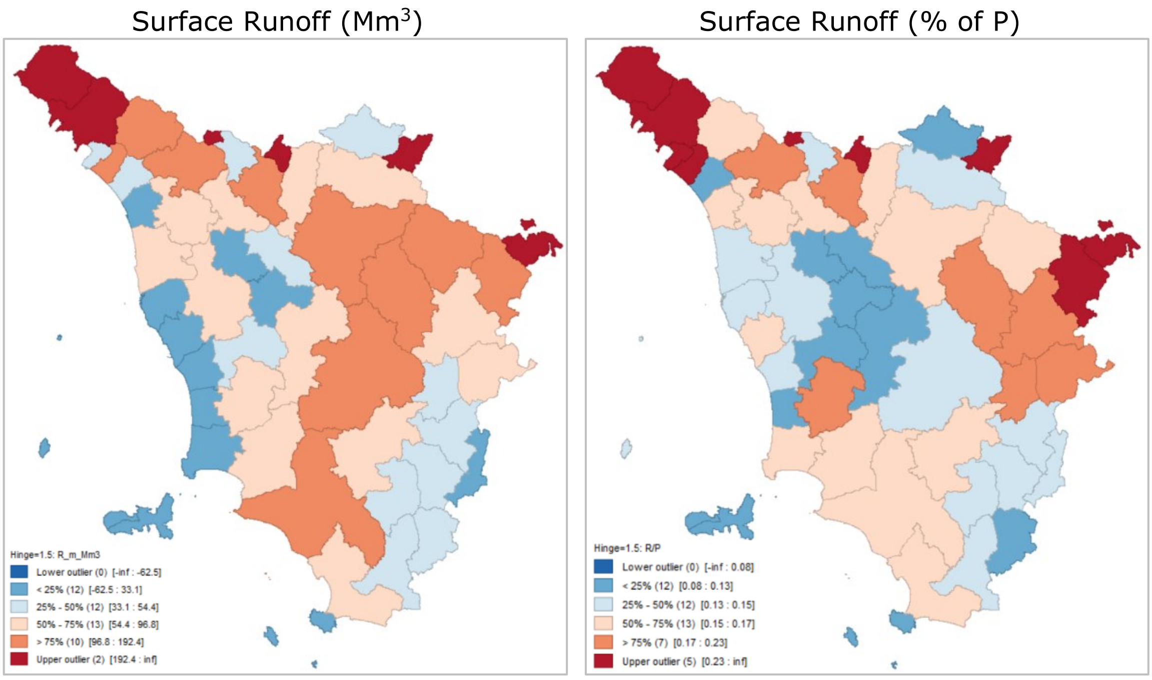

Source: own elaboration

2.1.5 Summary of average hydrology

Table 2-2 presents the spatial statistics of the average for each hydrological component estimated. Table 2-3 shows the same statistics considering each component as a percentage of the precipitation. Table 2-4 contains the volumes for each LLS.

The greatest variability corresponds to groundwater recharge, strongly influenced by the value of groundwater concessions in some subregions, which could extract recharged groundwater based on water from other subregions. This occurs to a lesser extent for surface water, most likely conditioned by the correction made to account for missing information.

Table 2-2. Spatial statistics for hydrological components (water volume)

Statistics	Precipitation	Evapotranspiration	Groundwater Recharge	Surface Runoff
Mean (Mm^3)	414	243	85	78
Standard Dev. (Mm^3)	275	163	102	79
Coef. Variation	66%	67%	120%	102%
Min. (Mm^3)	28	17	3	4
Max. (Mm^3)	1244	791	454	423

Source: own elaboration

Table 2-3. Spatial statistics for hydrological components (% of precipitation)

Statistics	Evapotranspiration	Groundwater Recharge	Surface Runoff
Mean	61%	21%	19%
Standard Dev.	14%	26%	13%
Coef. Variation	24%	121%	68%
Min.	37%	10%	13%
Max.	88%	166%	85%

Source: own elaboration

Table 2-4. Average value for hydrological components by LLS

SLL	Precipitation (Mm^3)	Evapotranspi-ration (Mm^3)	Groundwater Recharge (Mm^3)	Surface Runoff (Mm^3)
CARRARA	91	36	24	43
MASSA	159	60	33	136
PONTREMOLI	708	269	75	382
BARGA	724	271	454	127
CASTELNUOVO GARFAGNANA	708	266	109	111
LUCCA	534	234	95	81
PIETRASANTA	273	100	46	36
VIAREGGIO	210	91	347	32
MONTECATINI-TERME	357	177	53	55
PISTOIA	444	201	397	101
SAN MARCELLO PISTOIESE	289	112	31	41
BORGO SAN LORENZO	679	357	72	92
CASTELFIORENTINO	232	166	27	31
EMPOLI	251	174	35	33
FIRENZE	980	561	107	147
FIRENZUOLA	402	197	43	53
CASTAGNETO CARDUCCI	117	82	16	16
CECINA	163	112	30	23
LIVORNO	211	132	28	29
MARCIANA MARINA	28	17	3	4
PIOMBINO	211	168	39	31
PORTOFERRAIO	106	66	15	14
ROSIGNANO MARITTIMO	188	133	25	30
PISA	374	237	61	54
POMARANCE	405	242	45	76

SLL	Precipitation (Mm³)	Evapotranspi-ration (Mm³)	Groundwater Recharge (Mm³)	Surface Runoff (Mm³)
PONTEDERA	525	347	72	70
SAN MINIATO	245	148	39	32
VOLTERRA	301	218	39	40
AREZZO	543	345	130	97
BIBBIENA	747	360	394	110
CORTONA	313	235	60	58
MONTEVARCHI	634	368	89	120
SANSEPOLCRO	419	256	123	115
CHIUSI	144	105	16	20
MONTALCINO	551	399	58	82
MONTEPULCIANO	270	233	30	38
PIANCASTAGNAIO	291	206	33	40
POGGIBONSI	591	391	62	78
SIENA	1,134	791	121	155
SINALUNGA	207	167	48	42
CASTEL DEL PIANO	329	205	35	45
FOLLONICA	525	336	56	82
GROSSETO	934	745	123	161
MANCIANO	317	261	35	43
MONTE ARGENTARIO	47	29	5	6
ORBETELLO	410	360	56	60
PITIGLIANO	274	182	28	36
PRATO	428	201	136	70
extra	1,244	539	158	423

Source: own elaboration

Regional hydrological balances in Tuscany estimate the sum of evapotranspiration, groundwater recharge and surface runoff (EIR) to be 98% of precipitation (Braca, 2020, 2021). Figure 2-8 shows this ratio for each LLS, where imbalances are apparent due to the considerations made in the preceding sections. Figure 2-9 presents a map where it can be seen that the greatest differences occur in the northern sub-regions, where most of the surface and groundwater concessions are concentrated, given the high rainfall. In most of the LLS (42 out of 49) the value is in the range 75-125%.

Figure 2-8. Ratio between EIR and precipitation by LLS

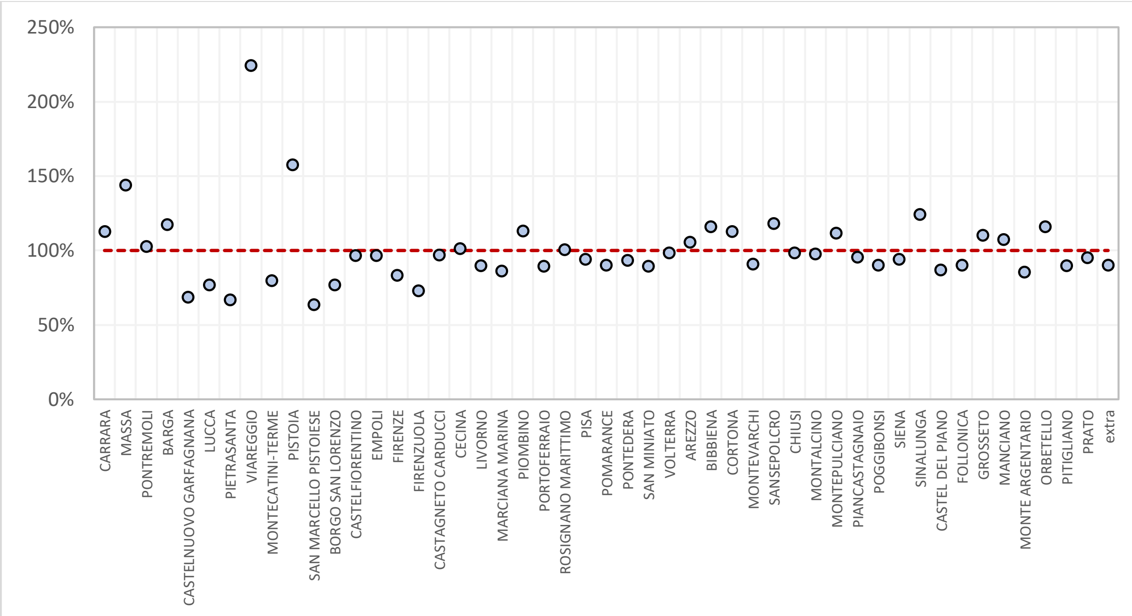

Source: own elaboration

Figure 2-9. Spatial heterogeneity of the ratio between EIR and precipitation

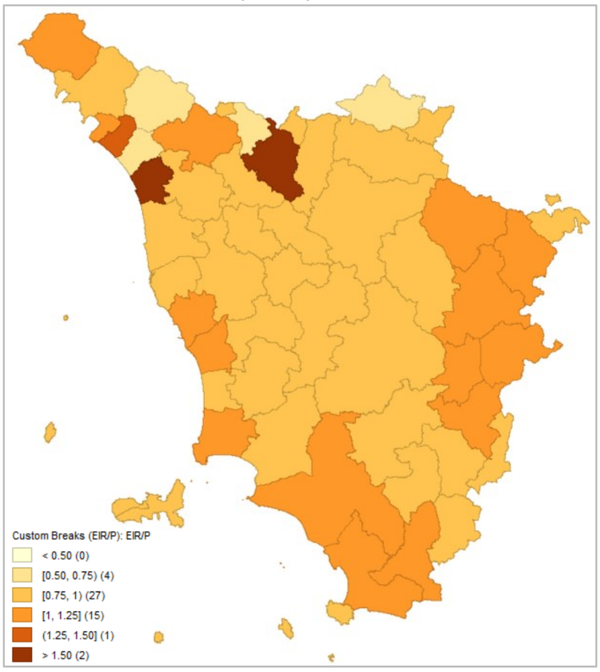

Source: own elaboration

The methodology used to verify the consistency of the disaggregation essentially perform the previous analysis (EIR as a percentage of precipitation) at the basin level. For this purpose, the subregions have been aggregated into 9 basins. It should be noted that 2 basins have only a part of it within the region (Tevere and Reno rivers) and that one of them corresponds to a set of islands, which may distort the results. However, 95% of the waters involved are associated with basins located entirely within the region. Figure 2-10 shows the overlap of the basins entirely located within the Tuscany region and the LLS.

Figure 2-10. River basins and LLS

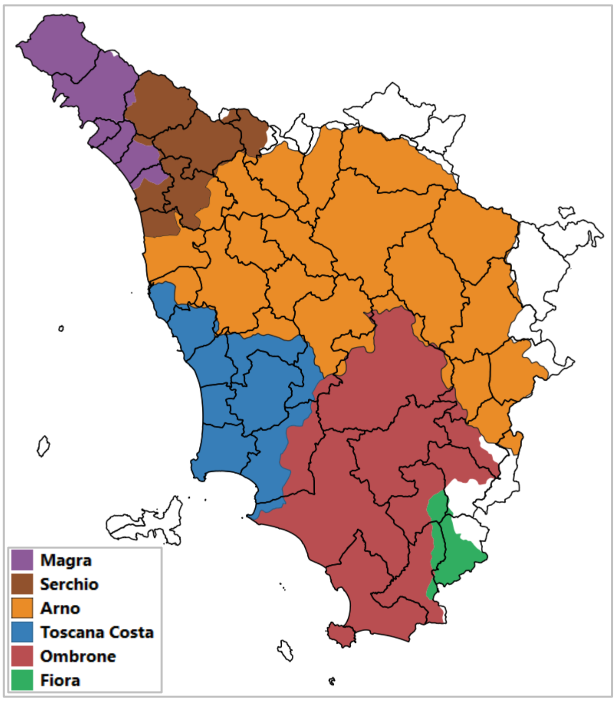

Source: own elaboration

Table 2-5 and Figure 2-11 show the aggregated results by watershed, where the consistency of the de-aggregation of the hydrological components for the 6 watersheds located entirely within the region can be appreciate. However, the results cannot be completely precise, due to the fact that, as shown in Figure 2-10, a watershed is not a perfect union of LLS, several of the subregions belong to two sub-basins. The criterion for attributing a subregion to a basin, in this case, has been to choose the basin where most of the LLS area is located.

Table 2-5. Hydrological components aggregated by river basin

Basin	P (Mm^3)	E (Mm^3)	I (Mm^3)	R (Mm^3)	EIR (Mm^3)	EIR/P
M. Marina - P. Ferraio	135	83	18	18	119	89%
Arno	8,031	4,801	1,840	1,258	7,899	98%
Fiora	274	182	28	36	246	90%
Magra	2,475	1,006	335	1,020	2,361	95%
Ombrone	4,013	2,995	465	593	4,052	101%
Reno	402	197	43	53	293	73%
Serchio	2,465	973	1,036	391	2,400	97%
Tevere	563	362	139	135	637	113%
Toscana Costa	1,911	1,292	250	299	1,841	96%

Source: own elaboration

Figure 2-11. Ratio EIR/P aggregated by river basin

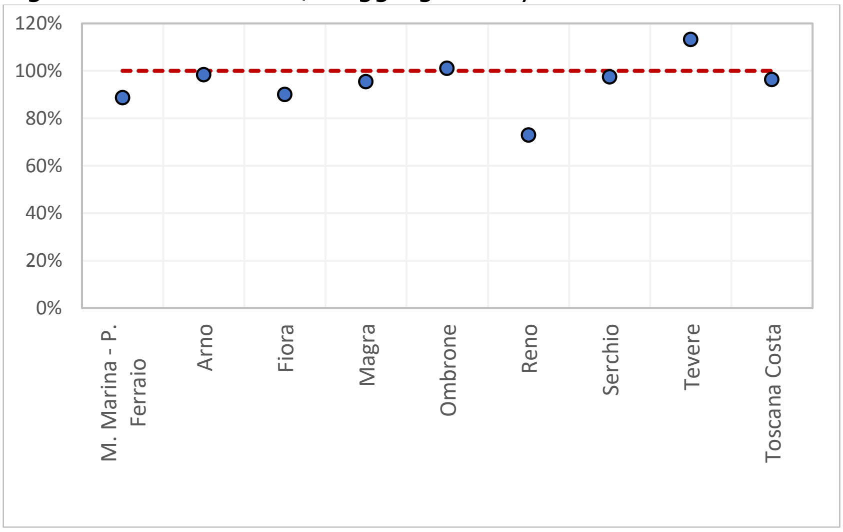

Source: own elaboration

2.2 Hydrological spatiotemporal variability

2.2.1 General aspects

In this section we propose a model to incorporate spatiotemporal variability to the mean hydrology estimated for each subregion in the preceding section. A spatial stochastic model is proposed to generate synthetic precipitation series based on weather station records in the region. Based on this model, N=100 synthetic precipitation series are generated and attributed to each LLS using the Voronoi polygon methodology. Based on these results and the average hydrological structure, a methodology is proposed to incorporate variability to the other hydrological components: evapotranspiration, groundwater recharge and surface runoff, by LLS.

2.2.2 A spatial stochastic model for precipitation

A spatial stochastic model is used to generate synthetic series of precipitation and evapotranspiration by LLS. These series allow to incorporate temporal variability together with the spatial structure into the mean hydrological components defined in the previous sections. The variability of groundwater recharge and surface runoff is characterised on the basis of the precipitation series.

A spatial stochastic model is the representation of a spatial and temporal random variable. It reproduces the main characteristics of the variable, in particular the mean, standard deviation and spatial correlation. Such a representation is obtained based on the analysis of temporal and spatial observations of the random variable. It is proposed a spatial stochastic model based on Rencher (2002) and Maity (2018).

Let Z be the vector of *N* variables. These random variables represent N different points in space and are dependent on each other at an instant in time. If the variable z_i is marginally normally distributed, with mean μ_i and variance σ_i, $\mathcal{N}(\mu_i, \sigma_i)$, the spatial model is defined by:

$$Z = \sum^{1/2} \cdot U + M \tag{2.6}$$

Where U is an *(N x 1)* vector with the standardised normal random variables, independent of each other. The *(N x 1)* vector *M* is the expected value of *Z, E(Z).* The *(N x N)* matrix ∑ is the variance-covariance matrix. These variables are defined as:

$$M = E(Z) \tag{2.7}$$

$$\sum = E\big((Z - M)(Z - M)^T\big) = \begin{bmatrix} \sigma_{11} & \sigma_{12} & \cdots & \sigma_{1N} \\ \sigma_{21} & \sigma_{22} & \cdots & \sigma_{2N} \\ \vdots & \vdots & \ddots & \vdots \\ \sigma_{N1} & \sigma_{N2} & \cdots & \sigma_{NN} \end{bmatrix} \tag{2.8}$$

Where σ_{ij} is the covariance between z_i and z_j, and the superscript *T* denotes the transposed matrix. The relationship between the covariance matrix ∑ and the cross-correlation matrix ϒ is:

$$\sum = \Gamma \cdot \Upsilon \cdot \Gamma = \begin{bmatrix} \sigma_1 & 0 & \cdots & 0 \\ 0 & \sigma_2 & \cdots & 0 \\ \vdots & \vdots & \ddots & 0 \\ 0 & 0 & \cdots & \sigma_N \end{bmatrix} \cdot \begin{bmatrix} \rho_{11} & \rho_{12} & \cdots & \rho_{1N} \\ \rho_{21} & \rho_{22} & \cdots & \rho_{2N} \\ \vdots & \vdots & \ddots & \vdots \\ \rho_{N1} & \rho_{N2} & \cdots & \rho_{NN} \end{bmatrix} \cdot \begin{bmatrix} \sigma_1 & 0 & \cdots & 0 \\ 0 & \sigma_2 & \cdots & 0 \\ \vdots & \vdots & \ddots & 0 \\ 0 & 0 & \cdots & \sigma_N \end{bmatrix} \tag{2.9}$$

Where each element of the ϒ (ρ_{ij}) is the coefficient of correlation between z_i and z_j. Γ is the diagonal (*N* x *N*) matrix of standard deviations of each z_i. The matrix $\sum^{1/2}$ is obtained through the Cholesky decomposition equation:

$$\sum^{1/2} (\sum^{1/2})^T = \sum \tag{2.10}$$

The above model can be used to generate synthetic series of any extension of the random variable at each of the *N* points. These synthetic series, Z^t, with *t=1, 2,...,T* where T is the length of the synthetic series, will reproduce mean values, variances, and spatial correlations. The equation for simulation of synthetic series is expressed as follows as:

$$Z^t = \sum^{1/2} \cdot U^t + M \tag{2.11}$$

Where U^t is a vector containing *N* standardized and independent normal variables. The vector U^t is generated from using a procedure for the simulation of normal random numbers.

2.2.3 Data for the model

We consider 42 precipitation stations located in the Tuscany region that meet the requirement of having 20 years with a reliable record of measurements (90% of daily data) in the period 1970-2010. Of these 42 stations, 21 correspond to those used in Bartolini's studies (2014, 2017) and the other 21 have been obtained for this study from SIR (2021).

Figure 2-12 shows a map with the precipitation stations considered for the model and Figure 2-13 presents a graphic with the number of years with reliable data by station.

Figure 2-12. Precipitation stations for the model

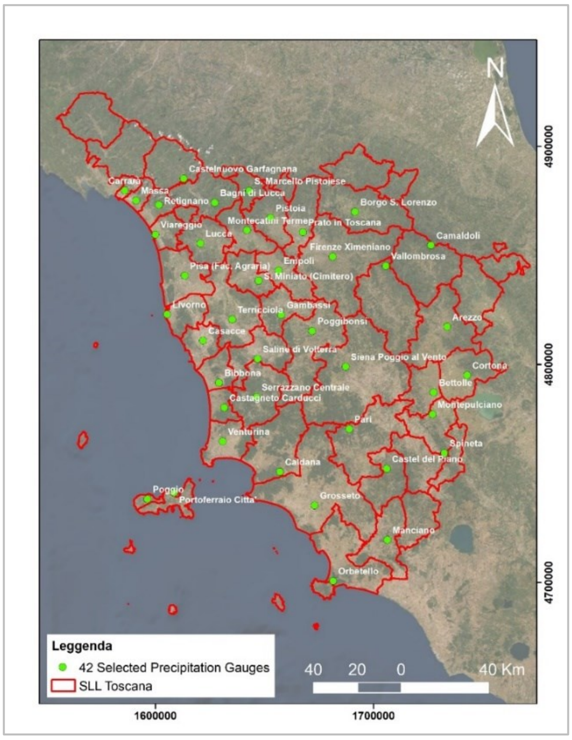

Source: own elaboration based on SIR (2021) and Bartolini (2013, 2017)

Figure 2-13. Years with reliable data by precipitation station

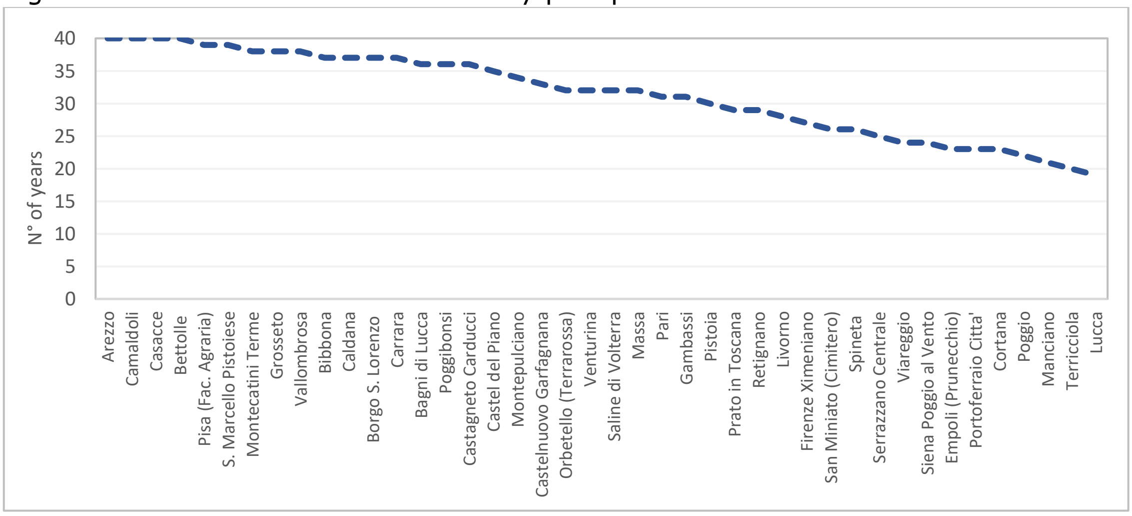

Source: own elaboration based SIR (2021)

2.2.4 Correlation matrix

Since the correlation matrix relates all variables, it must meet a requirement of consistency between the different correlations. A correlation matrix is consistent when is Positive-Definite, i.e., all eigenvalues of the correlation i.e., that all eigenvalues of the matrix are positive.

In general, the empirical correlation matrix is not the best estimator of the underlying correlations of the variables. Moreover, in many cases it does not even provide a feasible solution because it does not necessarily meet the requirement of being Positive-Defined. In general, if the series are of different lengths, the correlation matrix will not meet this requirement (Van Storch and Zweirs, 1999; Bras and Rodriguez-Iturbe, 1993).

As expected, the correlation matrix of annual precipitation correlations is not Positive-Defined. That is, they are not properly a correlation matrix. In order to estimate consistent correlation coefficients between the different pairs of stations using the observed data, a regression model was constructed that relates the degree of correlation between two stations to their differences in latitude, longitude and altitude.

The regression is:

$$\rho_{i,j} = 1 - \beta_h \left|\Delta H_{i,j}\right| - \beta_{lat} \left|\Delta Lat_{i,j}\right| - \beta_{lon} \left|\Delta Lon_{i,j}\right| \quad (2.12)$$

Where,

$\rho_{i,j}$	:	Correlation coefficient between precipitation station i and j
ΔH	:	Absolute value of the difference in altitude between precipitation station i and j (meters)
ΔLat	:	Absolute value of the difference in latitude between precipitation station i and j (meters, ΔUTM)
ΔLon	:	Absolute value of the difference in longitude between precipitation station i and j (meters, ΔUTM)

In this regression there is a large amount of data for calibration, as there are as many as pairs of stations, i.e. 42x41/2=861 points. The determination of the beta coefficients of the regression is also done using the least squares method weighted by the number of data in common between the pairs of series.

In this way, it is possible to smooth the correlation matrices and obtain the coherence that must exist between all the correlations, correcting the divergent correlations that are typically those that use few years of data for the calculation.

Figure 2-14 shows the estimated annual correlation matrix and the smoothed correlation matrix obtained with the proposed methodology.

Figure 2-14. Empirical and smoothed correlation matrix

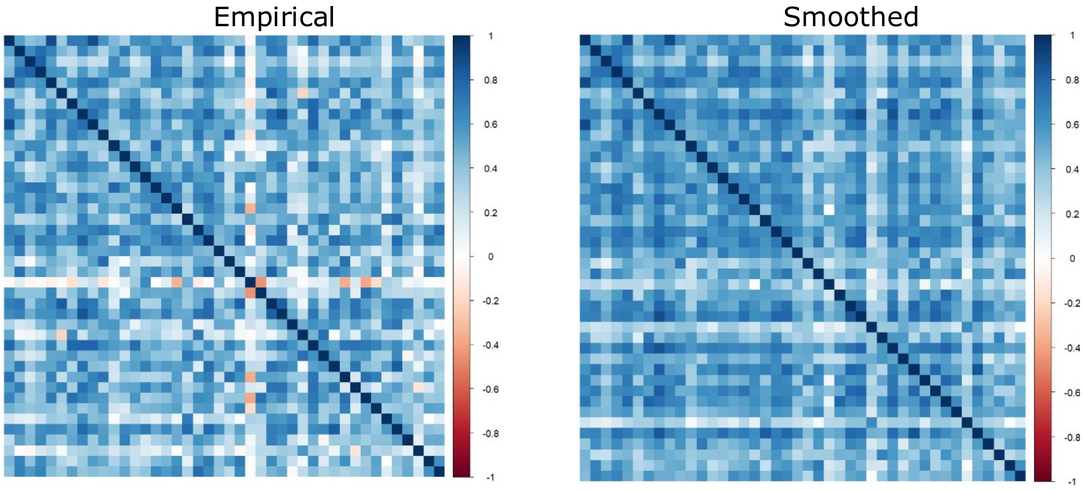

Source: own elaboration

2.2.5 Precipitation variability

As a result of the model, 42 series of N=100 years of precipitation are obtained. The model adequately represents the mean and variance of the original series (Figure 2-15).

Figure 2-15. Mean and standard deviation of generated precipitation series

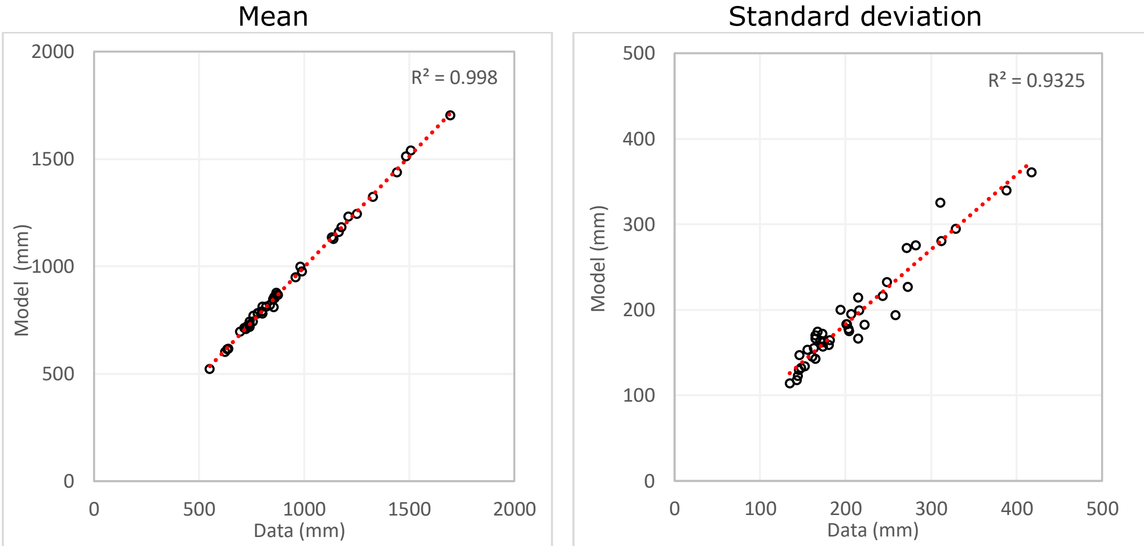

Source: own elaboration

The results are representative of 42 points in space, however, the objective is to characterize the precipitation of each subregion (for the same 100 years). The Voronoi polygon methodology (Te Chow, 2010) was used to determine the precipitation associated with each subregion. With this methodology the area of influence of each station has been determined, as shown in Figure 2-16.

Figure 2-16. Voronoi polygons for precipitation stations

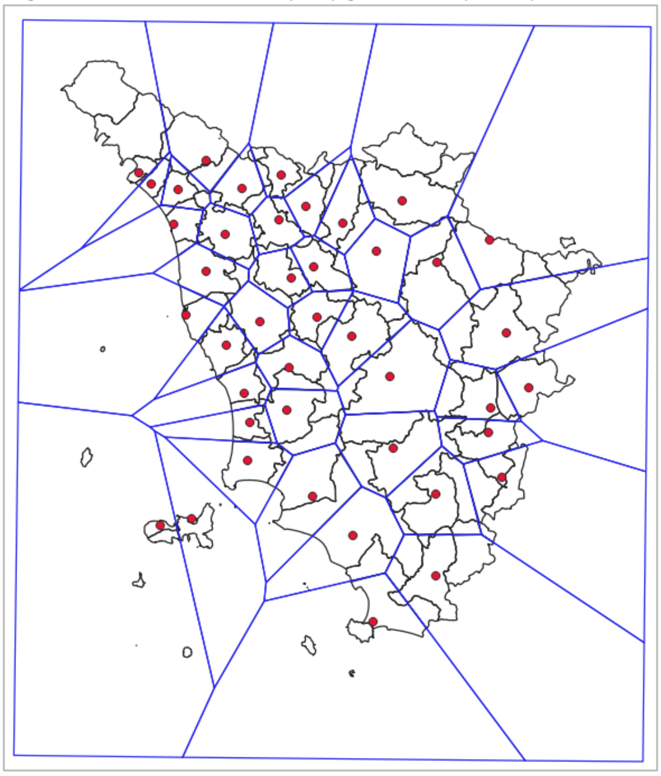

Source: own elaboration

The Voronoi polygons scheme allows to construct the matrix of weights W (42x49), where each element $W_{s,j}$ corresponds to the percentage of LLS's area associated to the influence area (polygon) of the precipitation station j. Then, the precipitation for year t and subregion s can be written as:

$$\mathcal{P}_t^s = \sum_{j}^{42} W_{s,j} \cdot \Omega_{j,t} \tag{2.13}$$

Where $\Omega_{j,t}$ is an element of the synthetic precipitation matrix (42x100) generated with the spatial stochastic model. Using the notation of the spatial stochastic model $\Omega = [Z^1, Z^2, \dots, Z^{100}]$.

2.2.6 Hydrological components variability

The precipitation determined for each LLS based on the methodology of the previous section allows incorporating variability to the mean precipitation ($\bar{P}^s$) estimated in section 2.1.1. Then the precipitation for year t and subregion s is obtained as:

$$P_t^s = \frac{\mathcal{P}_t^s}{\bar{\mathcal{P}}^s} \cdot \bar{P}^s \tag{2.14}$$

For groundwaters we define χ_I^s as the percentage of groundwater recharge of precipitation.

$$\chi_I^s = \frac{\bar{I}^s}{\bar{P}^s} \tag{2.15}$$

A random variation in this coefficient is generated conditional on years with above or below average precipitation, since groundwater recharge processes are more efficient in wetter years (Te Chow, 2010).

$$\tilde{\chi}_{I,t}^s = \chi_I^s \cdot v_{I,t} \tag{2.16}$$

The coefficient $v_{I,t}$ is defined based on a uniform variation dependent on parameter a_I, for which the values of the regional information are considered.

$$v_{I,t} = \begin{cases} unif\,[1-a_I, 1] & if \quad P_t^s \leq \bar{P}^s \\ unif\,[1, 1+a_I] & if \quad P_t^s > \bar{P}^s \end{cases} \tag{2.17}$$

Thus, the percentage of precipitation that is recharge and the groundwater recharge for year *t* and subregion *s* are defined by the following relationships:

$$\tilde{\chi}_{I,t}^s = \chi_I^s \cdot v_{I,t} \tag{2.18}$$

$$I_t^s = \tilde{\chi}_{I,t}^s \cdot P_t^s \tag{2.19}$$

The same procedure is used for the surface runoff variability, based on parameters $v_{R,t}$ and a_R.

$$\chi_R^s = \frac{\bar{R}^s}{\bar{P}^s} \tag{2.20}$$

$$\tilde{\chi}_{R_t}^s = \chi_R^s \cdot v_{R,t} \tag{2.21}$$

$$v_{R,t} = \begin{cases} unif\,[1-a_R, 1] & if \quad P_t^s \leq \bar{P}^s \\ unif\,[1, 1+a_R] & if \quad P_t^s > \bar{P}^s \end{cases} \tag{2.22}$$

$$R_t^s = \tilde{\chi}_{R,t}^s \cdot P_t^s \tag{2.23}$$

For the evapotranspiration variability it is considered that the balance between precipitation and the other hydrological components is maintained, according to the characteristics of each LLS. It is defined χ_{EIR}^s as the percentage of the three hydrological components over the precipitation and χ_E^s as the percentage of precipitation that is evapotranspiration for an average hydrological conditions.

$$\chi_{EIR}^s = \frac{\bar{E}^s + \bar{I}^s + \bar{R}^s}{\bar{P}^s} \tag{2.24}$$

$$\chi_E^s = \frac{\bar{E}^s}{\bar{P}^s} = \chi_{EIR}^s - \chi_I^s - \chi_R^s \tag{2.25}$$

Thus, the percentage of precipitation that is evapotranspiration and the evapotranspiration for year t and subregion s are:

$$\tilde{\chi}_{E,t}^s = \chi_{EIR}^s - \tilde{\chi}_{I,t}^s - \tilde{\chi}_{R\,t}^s \tag{2.26}$$

$$E_t^s = \tilde{\chi}_{E,t}^s \cdot P_t^s \tag{2.27}$$

2.2.7 Summary of hydrological variability

Figure 2-17 presents the coefficient of variation for each hydrological component and subregion, calculated based on the 100 hydrological years simulation.

Figure 2-17. Coefficient of variation for hydrological components

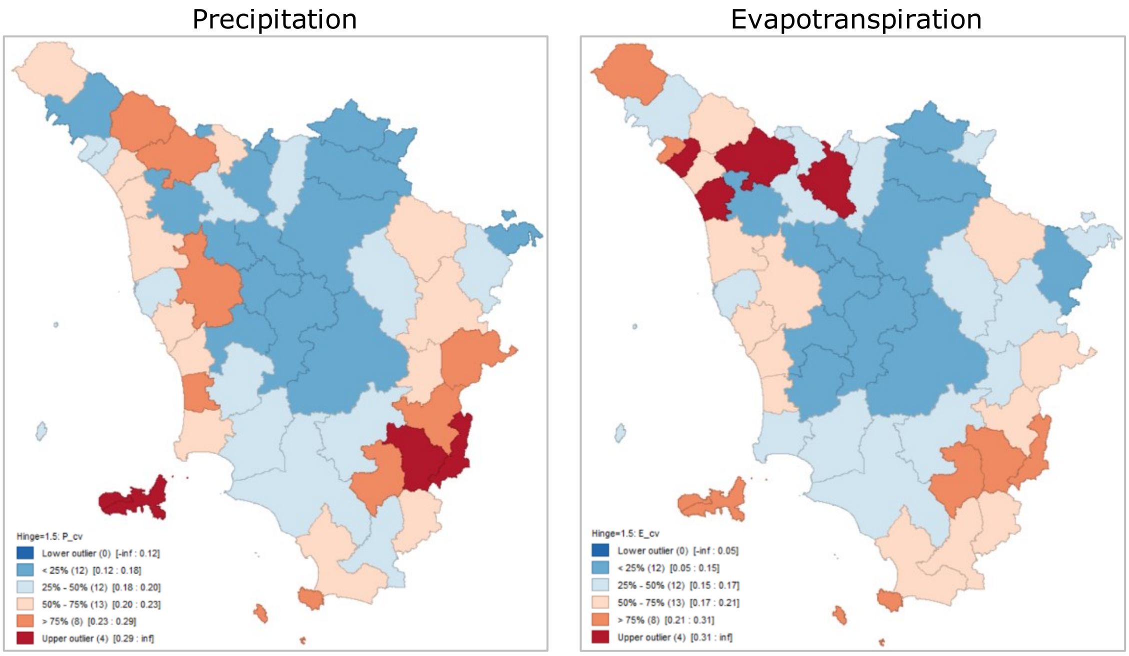

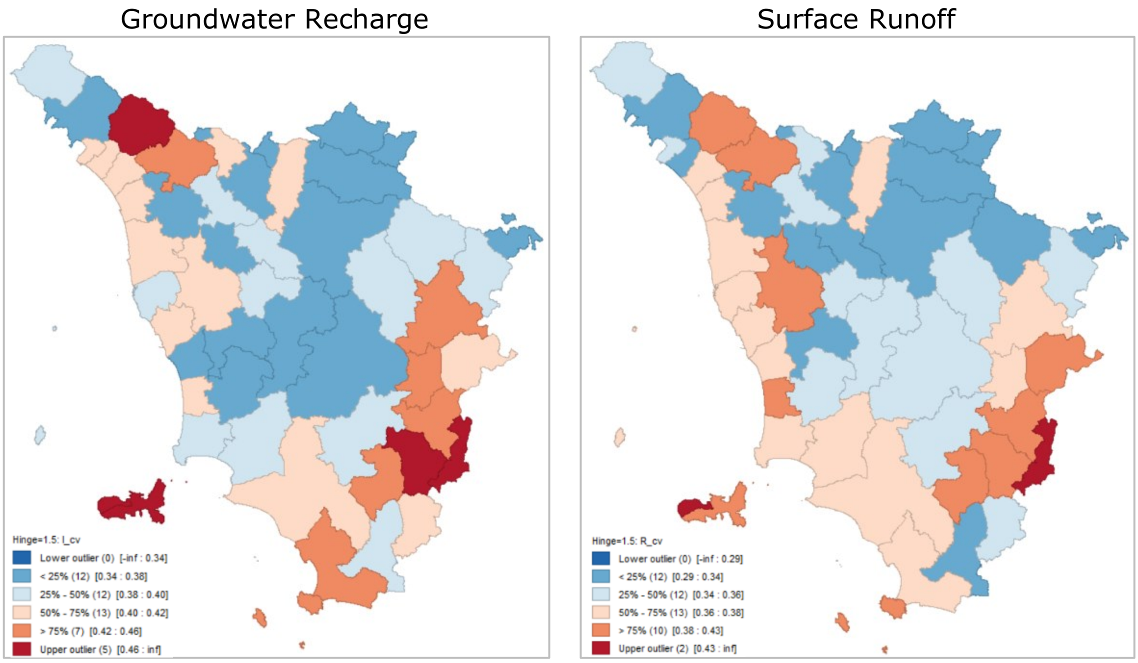

Source: own elaboration

Table 2-6 and 2-7 present the statistic for the regional model (Sturla and Rocchi, 2022) and for the aggregation at regional level of the model developed in the present study. It is observed that the model adequately reproduces the variability of the regional model.

Table 2-6. Regional model statistics

Reg Model	P	E	I	R
Mean (Mm^3)	20,269	11,892	4,155	3,803
S. Deviation (Mm^3)	3,084	1,129	1,258	1,157
C. Variation	15.2%	9.5%	30.3%	30.4%
Min (Mm^3)	14,027	9,164	1,935	1,704
Max (Mm^3)	27,161	14,270	7,331	8,124

Source: own elaboration based on (Sturla and Rocchi, 2022)

Table 2-7. Aggregated LLS model statistics

SLL Model	P	E	I	R
Mean (Mm^3)	20,269	11,890	4,155	3,803
S. Deviation (Mm^3)	2,965	1,066	1,149	1,220
C. Variation	14.6%	9.0%	27.6%	32.1%
Min (Mm^3)	12,798	8,705	1,970	1,547
Max (Mm^3)	27,227	14,925	6,633	6,843

Source: own elaboration

2.3 A climate change hydrological scenario

The spatial stochastic model for precipitation allows generating synthetic series by varying the mean and standard deviation associated with each meteorological station; generating the change in the simulated annual volume of precipitation for each LLS. In addition, it is possible to modify the mean values of the other hydrologic components in the model. However, the standard deviation of these other hydrologic components has an endogenous component in the model, which depends on the variability of precipitation, and an exogenous component associated with the incorporation of randomness in the structure of the mean hydrology.

Therefore, it is proposed to evaluate a climate change scenario by fitting the mean of all hydrological components and the standard deviation of precipitation. Given the lack of specific studies for the different basins of the region, for the effects of changes in mean values we consider the study of D'Oria et al. (2019) carried out for the northern Tuscany area, in particular for the period 2051-2060. These results are not very different from those obtained for the central coastal area of Tuscany by Pranzine et al. (2020). For the standard deviation of precipitation, the studies of Bartolini et al. (2014, 2017), Brunetti et al. (2006) and Fatichi and Caporali (2009) are also considered.

Although this climate change scenario assumes that the percentage changes are homogeneous in the region, it allows to simulate of the hydro-economic balance for a modified hydrological condition compared the base scenario.

Table 2-8 summarizes the climate change scenario considered; note that the standard deviation of evapotranspiration, groundwater recharge and surface runoff are endogenous to the model.

Table 2-8. Climate change scenario

Variabile	Media	D. Standard
Precipitazione	-3%	10%
Ruscellamento	-7%	fn (mod)
Ricarica	-8%	fn (mod)
Evapotraspirazione	4%	fn (mod)

Source: own elaboration

Table 2-9 presents the results of the N=100 synthetic series generated for the climate change scenario, aggregated at the regional level. Table 2-10 shows the percentage differences with respect to the scenario without climate change (base scenario). It can be seen that the standard deviation increases for all components except groundwater recharge, however, the coefficient of variation increases for all hydrological components in a range from 7.6% (groundwater recharge) to 13.7% (precipitation).

Table 2-9. Aggregated at regional scale of hydrology components for climate change scenario

Statistics	P	E	I	R
Mean (Mm^3)	19,661	12,366	3,823	3,537
S. Deviation (Mm^3)	3,266	1,225	1,135	1,279
C. Variation	16.6%	9.9%	29.7%	36.2%
Min (Mm^3)	11,427	8,178	1,765	1,354
Max (Mm^3)	27,331	15,940	6,233	6,361

Table 2-10. Differences between climate change scenario and base scenario (regional scale).

Statistics	P	E	I	R
Mean	-3.0%	4.0%	-8.0%	-7.0%
S. Deviation	10.2%	14.9%	-1.2%	4.8%
C. Variation	13.7%	10.0%	7.6%	12.8%
Min (Mm^3)	-10.7%	-6.1%	-10.4%	-12.5%
Max (Mm^3)	0.4%	6.8%	-6.0%	-7.0%

Source: own elaboration

3 HYDRO-ECONOMIC IRIO MODEL

3.1 IRIO table

The interregional input–output (IRIO) table is a top-down economic model, which uses interregional and inter-sectoral monetary transaction data to account for the interconnections of different industries in different regions.

The IRIO table used in this study was developed by the Tuscan Regional Institute for Economic Planning (IRPET, 2021). The original table included agriculture as a single industry. To better represent the role of agriculture in determining the overall water demand e its variability, the original single industry was disaggregated into 8 sub-sectors, according to the Farm Types (FT) classification defined at European Union level and used in economic analyses to support sector policies (Common Agricultural Policy). The disaggregation of Agriculture account in the IO table into subsectors started with a breakdown of regional agricultural output at the municipal level using both secondary data published by ISTAT and using year georeferenced information on cultivated crops and irrigated areas at a single-field geographic scale, reporting administrative data generated by the implementation of agricultural policy. The value added produced by each subsector of regional agriculture was estimated applying an average value added/output ratio by Farm Type. The statistical information used to define specific ratios for each FT is the sample of farms surveyed in Italy by the National Research Council Center for Agriculture (CREA) under the European Farm Accounting Data Network (FADN). The FADN Public Database (http://ec.europa.eu/agriculture/rica/index.cfm) provides data on the average composition of farms' output and production costs at the national and regional levels, with a breakdown by FT and by economic size of the farm.

Once obtained output and value added estimates at the municipality level, they were reaggregated to obtain the agriculture account at the level of Local Labour Systems. A detailed description of definition adopted, data used and procedures in the disaggregation of Agriculture by FT can be found in (Rocchi and Sturla, 2021).

The final multi-regional matrix is referred to year 2017 and contains 53 economic sectors, 49 LLSs, 5 components of the internal final demand and 4 components of external final demand (Rest of Italy and Rest of the World).

Figure 3-1 shows a scheme of the IRIO table of Tuscany. Each block on the main diagonal in the central part representing the intermediate flows, correspond to the IO matrix of a single LLS, while the blocks outside the main diagonal include flows of intermediate inputs traded among production activities in different LLSs. The balance of each LLS/Industry account is ensured by the flows recorded in the matrices of final demand (disaggregated by LLS for final consumptions), value added formation and by vectors of external trade (with the rest of Italy and the Rest of the World.

Figure 3-1. Structure of the IRIO table of Tuscany

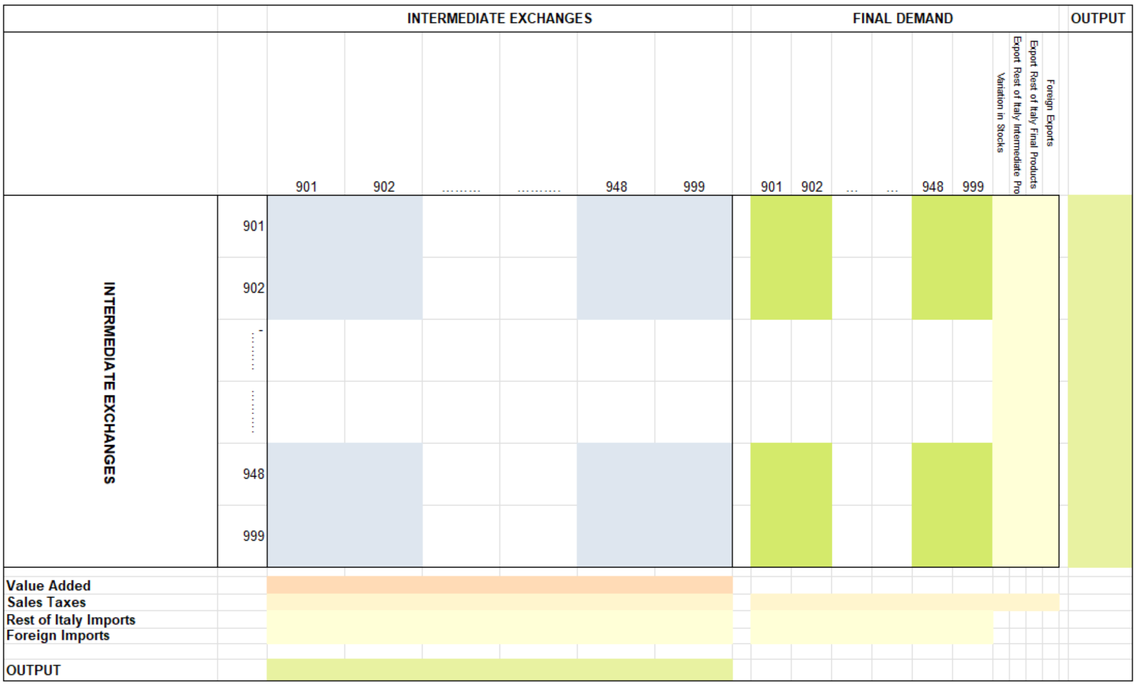

Source: own elaboration based on IRPET (2021)

For the purposes of assessing the hydro-economic balance of local economies, the relevant information corresponds to the domestic production associated with each LLS. However, given that the opportunity cost of the hydro-economic equilibrium is estimated, the flows between sub-regions are of great importance, i.e., the reduction of production in one sub-region has effects on production in other sub-regions.

3.2 Extended demand and EWEI indicator

3.2.1 The general model

Assuming the number of regions is *n*, and for each region there are *m* industries, the mathematical structure of an interregional input–output system consists of *(m x n)* linear equations (Isard et al., 1960). They show the contribution of the production of one sector in one region to the intermediate and final consumption of all the sectors of all the regions in the form of monetary transactions of goods and services.

The environmentally extended interregional input-output model (Miller and Blair, 2009) allows to calculate the total environmental resource used by an economic system:

$$E = C^T \cdot x \tag{3.1}$$

Where *E* is the *(mn x 1)* vector of the environmental resources used by subregion and industry, x is the *(mn x 1)* vector of outputs and *C* is the *(mn x 1)* vector of environmental resource use intensities. Superscript *T* denotes the transpose.

The vector x can be expressed in function of the technical coefficients *(mn x mn)* matrix A and the *(mn x 1)* vector y of total final demand

$$x = (I - A)^{-1} \cdot y \tag{3.2}$$

Defining $L = (I - A)^{-1}$ as the interregional Leontief inverse *(mn x mn)* matrix yields

$$E = C^T \cdot L \cdot y \tag{3.3}$$

3.2.2 Extended demand

For the purposes of this study, the environmental resource is water. The extended water demand is defined as withdrawals (blue and green water) minus discharges plus the water requirements for dilution (grey water).

The extended demand of water *(n x 1)* vector for each subregion (e_k^s) could be expressed as:

$$e_k^s = (\widehat{f_k^s} - \widehat{r_k^s} + \widehat{w_k^s}) \cdot L^s \cdot y \tag{3.4}$$

Where the L^s *(m x mn)* matrix corresponds to the Leontief inverse matrix blocks associated with production in the subregion *s* , *y (mn x 1)* vector is the final demand and f_k^s, r_k^s and correspond to the (*m x 1)* vectors (in m³/€) of intensity coefficients for withdrawals, discharges and water for dilution, respectively, by water body *k* (groundwater, surface water and soil moisture) in subregion s. The hat symbol indicates the diagonalization of the vector.

When temporal hydrological variability is considered, the water use coefficients change according to the components of the hydrologic cycle. Let us first define the water extended demand for the subregion *s* associated with water body *k*, industry *i* and year *t* (for notation simplicity we use x^s instead of $L^s y$)*:*

$$e_{k,i,t}^s = (f_{k,i,t}^s - r_{k,i,t}^s + w_{k,i,t}^s) \cdot x_i^s \tag{3.5}$$

Withdrawal coefficients will change for agricultural sectors, due to variations in soil moisture availability, which will imply higher withdrawals from surface and groundwater bodies when demand for green water exceeds supply for agriculture. Discharge coefficients also change because withdrawing water from surface water and groundwater involves considering irrigation losses. The dilution water requirement coefficients will change for all sectors discharging polluted water, depending on runoff, groundwater recharge, which define the concentration of pollutant in the receiving bodies. The latter coefficients depend indirectly on soil moisture due to their estimation as a function of discharge volume.

The above will be explained and formalized in later sections, however, a general scheme for extended demand dependence in hydrology is defined here.

Equations (3.6), (3.7) and (3.8) present the water use coefficients, each of which can be written as a function of its deterministic value (Rocchi and Sturla, 2021) plus a time-varying term, which depends on hydrological components:

$$f_{k,i,t}^{s} = f_{k,i}^{s} + \mathcal{F}_{k,i,t}^{s}(P_t^s, E_t^s) \tag{3.6}$$

$$r_{k,i,t}^{s} = r_{k,i}^{s} + \mathcal{R}_{k,i,t}^{s}\,(P_t^s, E_t^s) \tag{3.7}$$

$$w_{k,i,t}^{s} = w_{k,i}^{s} + \mathcal{H}_{k,i,t}^{s}[I_t^s, R_t^s, \mathcal{R}_{k,i,t}^{s}(P_t^s, E_t^s)] \tag{3.8}$$

Where I_t^s, R_t^s and S_t^s are the groundwater recharge, the runoff and the soil moisture, respectively, in subregion *s* for year *t*, obtained with the hydrological model.

Using equations (3.6) to (3.8) it is possible to write a general form to the extend demand associated with the water body *k*, the industry *i* and the year *t*.

$$e_{k,i,t}^{s} = e_{k,i}^{s} + \left[\mathcal{F}_{k,i,t}^{s}(P_t^s, E_t^s) + \mathcal{R}_{k,i,t}^{s}\,(P_t^s, E_t^s) + \mathcal{H}_{k,i,t}\left[I_t^s, R_t^s, \mathcal{R}_{k,i,t}(P_t^s, E_t^s)\right]\right] \cdot x_i^s \tag{3.9}$$

Note that $\mathcal{F}_{k,i,t}^{s}(P_t^s, E_t^s) = 0$ and $\mathcal{R}_{k,i,t}^{s}\,(P_t^s, E_t^s) = 0$ for non-agricultural sectors, and $\mathcal{H}_{k,i,t}[I_t^s, R_t^s, \mathcal{R}_{k,i,t}(P_t^s, E_t^s)] = 0$ for non-discharging sectors.

3.2.3 EWEI Indicator

The extended water exploitation index (EWEI) is defined as the ratio between the water extended water demand and the feasible water supply for a year *t*. Feasible supply considers environmental, technical and institutional constrains to the use of water (Sturla and Rocchi, 2021).

$$EWEI_t = \frac{\sum_{i=1}^{N}\sum_{k=1}^{2}(f_{k,i,t}^{s} - r_{k,i,t}^{s} + w_{k,i,t}^{s}) \cdot x_i^s}{I_t^{s,feas} + R_t^{s,feas}} \quad (3.10)$$

where the sum considers groundwater and surface water, $k = \{1,2\}$. $I_t^{s,feas}$ and $R_t^{s,feas}$, correspond the groundwater and surface water feasible supply:

$$I_t^{s,feas} = \left\{ \begin{array}{cc} \bar{I}^s(1-B^s) & if \;\; I_t^s < \bar{I}^s(1-B^s) \\ \bar{I}^s(1+B^s) & if \;\; I_t^s > \bar{I}^s(1+B^s) \\ I_t^s & if \;\; I_t^s \in [\bar{I}^s(1-B^s), \bar{I}^s(1+B^s)] \end{array} \right\} \quad (3.11)$$

$$R_t^{s,feas} = \left\{ \begin{array}{cc} R_t^s - E^s\bar{R}^s & if \;\; E\bar{R}^s \leq R_t^s \leq M^s\bar{R}^s + E\bar{R}^s \\ M^s\bar{R}^s & if \;\; R_t^s > M^s\bar{R}^s + E\bar{R}^s \\ 0 & if \;\; R_t^s < E\bar{R}^s \end{array} \right\} \quad (3.12)$$

where,

I_t^s	:	Groundwater recharge volume in year t in subregion *s*
$\bar{I}^s$	:	Long-term groundwater recharge volume in subregion *s*
B^s	:	Parameter defining the range of groundwater feasible availability in subregion *s*
R_t^s	:	Runoff volume in year t (multivariate model)
$\bar{R}^s$	:	Long-term runoff volume in subregion *s*
E^s	:	Ecological flow as proportion of mean runoff in subregion *s*
M^s	:	Maximum volume of concessions as proportion of mean runoff in subregion *s*

For this study we use a value of $B^s = 13\%$ and $E^s = 20\%$ for all subregions (Rocchi and Sturla, 2021). The value of M^s depends on the concessions value by subregions, estimated based on information from SIR (2021) and corrected with the proposed methodology based on the missing data estimates of Venturi et al. (2014).

3.3 Variability of agricultural water demand

Following the methodology of Sturla and Rocchi (2022), the lack of precipitation is used as a proxy for the lack of soil moisture, i.e. green water supply, which must be replaced by blue water (surface and groundwater). In addition, the variation of irrigation water demand based on evapotranspiration is considered, because the irrigation water requirement coefficients correspond to average hydrometeorological conditions.

Since the agricultural sectors contain both crops and livestock activities (zootechnics), the crop component only is considered for the hydrological variability effects. The withdrawal and discharge deterministic coefficients of the agricultural sectors can be broken down into the part requiring irrigation (irrigated crops and non-irrigated but potentially irrigated crops) and the part associated with livestock:

$$f_{k,i}^{s} = f_{k,i}^{s,irr} + f_{k,i}^{s,liv} \tag{3.13}$$

$$r_{k,i}^{s} = r_{k,i}^{s,irr} + r_{k,i}^{s,liv} \tag{3.14}$$

In this section, subscript *i* refers only to crop production activities.

The following subsections details the methodology used to modify the water withdrawal and discharge coefficients for a year, depending on the need to substitute green water with blue water (modelled using precipitation variability) and the variability of blue water requirements in irrigated agriculture (modelled using evapotranspiration variability).

3.3.1 Substitution of green water with blue water

Let define $\mathcal{E}_t^s$ as the ratio of the precipitation in year t (P_t^s) to the average precipitation ($\bar{P}^s$) for subregion *s*.

$$\mathcal{E}_t^s \equiv \frac{P_t^s}{\bar{P}^s} \tag{3.15}$$

Let define $TP_{i,t}^s$ as the additional groundwater and surface water withdrawals by the agricultural sector i, subregion s, year t, due to changes in precipitation.

$$TP_{i,t}^s = \begin{cases} (1-\mathcal{E}_t^s)\cdot f_{hc,i}^{s,irr}\cdot x_i^s\ \cdot\gamma_i^s & if\ \ \mathcal{E}_t^s < 1 \\ 0 & if\ \ \mathcal{E}_t^s \geq 1 \end{cases} \tag{3.16}$$

where,

$$\gamma_i^s = \frac{1}{1-\rho_i^s} \tag{3.17}$$

The parameter ρ_i^s corresponds to the losses associated with the irrigation process in the agricultural sector *i* of subregion *s*. When irrigation is used to supply agricultural requirements, an additional water withdrawal due to irrigation efficiency must be considered.

The term $f_{hc,i}^{s,irr}\cdot x_i^s$ corresponds to the water withdrawals from hydrological cycle for the average year in the agricultural sector *i* of subregion *s* (deterministic case).

To disaggregate the need for additional irrigation between groundwater and surface water, consider the following parameters:

δ_i^s: proportion of groundwater irrigation in sector *i* of subregion *s*
η_i^s: proportion of surface water irrigation in sector *i* of subregion *s*

where,

$$\delta_i^s = \frac{f_{gw,i}^{s,irr}}{f_{gw,i}^{s,irr} + f_{sw,i}^{s,irr}} \tag{3.18}$$

$$\eta_i^s = \frac{f_{sw,i}^{s,irr}}{f_{gw,i}^{s,irr} + f_{sw,i}^{s,irr}} \tag{3.19}$$

Then, $TP_{i,gw,t}^s$ and $TP_{i,sw,t}^s$ correspond to the increase in the withdrawals of groundwater and surface water in sector i of subregion s for year t, respectively, to make up for the deficit of green water:

$$TP_{i,gw,t}^s = \begin{cases} \delta_i^s \cdot (1-\mathcal{E}_t^s) \cdot f_{hc,i}^{s,irr} \cdot x_i^s \cdot \gamma_i^s & if\ \mathcal{E}_t^s < 1 \\ 0 & if\ \mathcal{E}_t^s \geq 1 \end{cases} \tag{3.20}$$

$$TP_{i,sw,t}^s = \begin{cases} \eta_i^s \cdot (1-\mathcal{E}_t^s) \cdot f_{hc,i}^{s,irr} \cdot x_i^s \cdot \gamma_i^s & if\ \mathcal{E}_t^s < 1 \\ 0 & if\ \mathcal{E}_t^s \geq 1 \end{cases} \tag{3.21}$$

3.3.1 Change in blue water irrigation requirements

Let define θ_t as the ratio of the evapotranspiration in year *t* (E_t^s) to the average evapotranspiration ($\bar{E}^s$):

$$\theta_t^s \equiv \frac{E_t^s}{\bar{E}^s} \tag{3.22}$$

The change in the use of groundwater and surface water by agriculture due to interannual changes in evapotranspiration is defined as:

$$TE_{i,t}^s = (\theta_t^s - 1) \cdot \left(f_{gw,i}^{s,irr} \cdot x_i^s + f_{sw,i}^{s,irr} \cdot x_i^s\right) \tag{3.23}$$

The terms $f_{gw,i}^{s,irr} \cdot x_i^s$ and $f_{sw,i}^{s,irr} \cdot x_i^s$ corresponds to the water withdrawals from groundwater and surface water for the deterministic case.

The additional withdrawals of groundwater and surface water are written as:

$$TE_{i,gw,t}^{s} = \delta_i^s \cdot (\theta_t^s - 1) \cdot f_{gw,i}^{s,irr} \cdot x_i^s \tag{3.24}$$

$$TE_{i,sw,t}^{s} = \eta_i^s \cdot (\theta_t^s - 1) \cdot f_{sw,i}^{s,irr} \cdot x_i^s \tag{3.25}$$

$TE_{i,gw,t}^{s}$ and $TE_{i,sw,t}^{s}$ correspond to the increase (decrease) in the withdrawals of groundwater and surface water in sector *i* for year *t*, due to the increase (decrease) in blue water irrigation requirements.

3.3.2 Coefficients with hydrological variability

Adding the effect of precipitation (equations (3.20) and (3.21)) and evapotranspiration (equations (3.24) and (3.25)), and dividing by x_i^s, yields the variable component of the withdrawal coefficient for groundwater and surface water in agricultural sectors:

$$\mathcal{F}_{gw,i,t}^{s}(P_t^s, E_t^s) = \begin{cases} \delta_i^s \left[\left(\frac{\bar{P}^s - P_t^s}{\bar{P}^s}\right) \cdot f_{hc,i}^{s,irr} \cdot \gamma_i^s + \left(\frac{E_t^s - \bar{E}^s}{\bar{E}^s}\right) \cdot f_{gw,i}^{s,irr}\right] & if\ \mathcal{E}_t^s < 1 \\ \delta_i^s \left[\left(\frac{E_t^s - \bar{E}^s}{\bar{E}^s}\right) \cdot f_{gw,i}^{s,irr}\right] & if\ \mathcal{E}_t^s \geq 1 \end{cases} \tag{3.26}$$

$$\mathcal{F}_{sw,i,t}^{s}(P_t^s, E_t^s) = \begin{cases} \eta_i^s \left[\left(\frac{\bar{P}^s - P_t^s}{\bar{P}^s}\right) \cdot f_{hc,i}^{s,irr} \cdot \gamma_i^s + \left(\frac{E_t^s - \bar{E}^s}{\bar{E}^s}\right) \cdot f_{sw,i}^{s,irr}\right] & if\ \mathcal{E}_t^s < 1 \\ \eta_i^s \left[\left(\frac{E_t^s - \bar{E}^s}{\bar{E}^s}\right) \cdot f_{sw,i}^{s,irr}\right] & if\ \mathcal{E}_t^s \geq 1 \end{cases} \tag{3.27}$$

For the withdrawal coefficient associated with the hydrologic cycle, its variable component (negative) is:

$$\mathcal{F}_{hc,i,t}^{s}(P_t^s) = \begin{cases} \left(\frac{P_t^s - \bar{P}^s}{\bar{P}^s}\right) \cdot f_{hc,i}^{s,irr} & if\ \mathcal{E}_t^s < 1 \\ 0 & if\ \mathcal{E}_t^s \geq 1 \end{cases} \tag{3.28}$$

In this work we assume that discharges from the agricultural sector are entirely directed to groundwater. Considering α_i as the proportion of the discharged water with respect to the groundwater and surface water withdrawals for the agricultural sector *i*, it is obtained that the additional discharges due to hydrologic variability are:

$$\mathcal{R}_{gw,i,t}^{s}(P_t^s, E_t^s) = [\mathcal{F}_{gw,i,t}^{s}(P_t^s, E_t^s) + \mathcal{F}_{sw,i,t}^{s}(P_t^s, E_t^s)] \cdot \alpha_i \tag{3.29}$$

$$\mathcal{R}_{sw,i,t}^{s}(P_t^s, E_t^s) = 0 \tag{3.30}$$

where,

$$\alpha_i^s = \frac{r_{gw,i}^{s,irr}}{f_{gw,i}^{s,irr} + f_{sw,i}^{s,irr}} \tag{3.31}$$

Since hydrologic variability influences only the withdrawal and discharge coefficients of the agricultural sectors, the above equations are sufficient to characterize equations (3.6) and (3.7) of the input-output model.

Note that parameters $(\delta_i^s, \eta_i^s, \alpha_i^s)$ are all defined based on the average hydrological conditions, that is, for the deterministic situation. It is assumed an irrigation losses in groundwater and surface water equal to $\rho_i^s = 30\%$, obtaining $\gamma_i^s = 1.42$, for all agricultural sectors and subregions.

3.4 Variability of water demand for dilution

The deterministic coefficient $w_{k,i}^s$ of equation (9) was calculated by Rocchi and Sturla (2021) with a mixing model based on a mass balance of COD concentration with intermediate chemical reaction, improving a previous versions (Xie, 1996; Guan and Hubacek, 2008).

The $w_{k,i,t}^s$ of equation (3.8), for this study, is calculated based on the same model, but considering time dependence and two endogenous effects:

- Discharges volumes from the agricultural sector depend on precipitation (P_t^s) and evapotranspiration (E_t^s), as discussed in the preceding section.
- The COD concentration in receiving water bodies depends on groundwater recharge (I_t^s) and runoff (R_t^s) .

The coefficients of water requirements for dilution by water body *k* and industry I for the year *t*, are expressed as:

$$w_{k,i,t}^s = \frac{u_{k,i,t}^s}{x_i^s} \tag{3.32}$$

Where, $u_{k,i,t}^s$ (m^3/year) is the water for dilution, which is calculated with the following mixing model:

$$u_{k,i,t}^s = \left[\frac{k_{2_k} \cdot c_{p_{k,i,t}}^s - c_{s_{k,t}}}{k_{1_k} \cdot c_{s_{k,t}}^s - c_{0_{k,t}}^s}\right] r_{k,i,t}^s \cdot x_i^s \tag{3.33}$$

where,

k_{1_k}	:	total reaction rate of pollutants after entering the water body *k*
k_{2_k}	:	pollution purification rate before entering the water body *k*
$r^s_{k,i,t} \cdot x^s_i$	:	discharges into the water body *k* associated with economic sector *i* and subregion *s,* for year t
$c_{p}{}^s_{k,i,t}$	:	COD concentration in the discharges to the water body *k* associated with economic sector *i* and subregion *s*
$c_{s}{}^s_{k,t}$	:	Standard COD concentration in water body *k* and subregion *s* for year *t*
$c_{0}{}^s_{k,t}$	:	COD concentration in water body *k* and subregion *s* for year t

Note that $r^s_{k,i,t} = r^s_{k,i} + \mathcal{R}^s_{k,i,t}(S^s_t)$ (equation (3.7)) is completely defined by the hydrological variability in the agricultural sectors. This is the first endogenous component.

The other endogenous component corresponds to $c_{0}{}^s_{k,t}$, the COD concentration in the water bodies. We propose an expression for this term that takes into account decreases in COD concentration due to wetter hydrology and increases in COD concentration due to drier hydrology; this is based on the fact that the discharge of organic matter (whose indicator used is COD) depends on the economic system, which, in the case of this work, is considered constant, or more generally, its variability is much smaller than the hydrologic variability.

The variable $\pi^s_{k,t}$ is defined by the hydrological model, for groundwater and surface water, like the ratio between the natural supply (hydrological model) in year *t* and the long-term supply, for the water body *k* and subregion *s*:

$$\pi^s_{gw,t} \equiv \frac{I^s_t}{\bar{I}^s} \tag{3.34}$$

$$\pi^s_{sw,t} \equiv \frac{R^s_t}{\bar{R}^s} \tag{3.35}$$

Let define the following parameters:

$c_{0}{}^{min}_k$	:	Minimum concentration in water body *k*
$c_{0}{}^{max}_k$	:	Maximum concentration in water body *k*
$c_{0}{}^{mean}_k$	:	Mean concentration in water body *k*
π^{min}_k	:	Ratio of minimum volume to average volume in water body *k*
π^{max}_k	:	Ratio of maximum volume to average volume in water body *k*
π^{mean}_k	:	Equal to 1 by definition

A linear model is constructed to represent the relationship between the concentration in water bodies before discharge and hydrology (both surface and groundwater). The following linear relation is considered for $c_{0_{k,t}} \in (c_{0_k}^{min}, c_{0_k}^{max})$:

$$c_{0_{k,t}}^s = a \cdot \pi_{k,t}^s + b \qquad (3.36)$$

where,

$$a = \frac{c_{0_k}^{max} - c_{0_k}^{min}}{\pi_k^{min} - \pi_k^{max}}$$

$$b = c_{0_k}^{mean} - a$$

For concentrations below the minimum and above the maximum, the ratio of the maximum concentration to the runoff or recharge level indicator (hydrology) is considered constant. Thus, the linear function is defined as follows:

$$c_{0_{k,t}}^s = \begin{cases} c_{0_k}^{min} & if \quad \pi_{k,t} \le \pi_k^{min} \\ a \cdot \pi_{k,t} + b & if \quad \pi_k^{min} < \pi_{k,t}^s < \pi_k^{max} \\ c_{0_k}^{max} & if \quad \pi_{k,t} \ge \pi_k^{max} \end{cases} \qquad (3.37)$$

When the concentration in the water bodies ($c_{0_{k,t}}^{\ s}$) is higher than the standard concentration in average conditions (c_{s_k}), the standard concentration for the year *t* in subregion *s* ($c_{s_{k,t}}^{\ s}$) is considered to be that of the water body, since in the model the water for dilution come from the hydrological system. Then:

$$c_{s_{k,t}}^s = \begin{cases} c_{s_k}^s & if \quad c_{0_{k,t}}^s \le c_{s_k} \\ c_{0_{k,t}}^s & if \quad c_{0_{k,t}}^s > c_{s_k} \end{cases} \qquad (3.38)$$

With equations (3.37) and (3.38) it is calculated $u_{k,i,t}$ in equation (3.33) and $w_{k,i,t}^s$ in equation (3.32). Thus, the additional water for dilution with hydrological variability can be calculated as the difference between the stochastic model coefficient ($w_{k,i,t}^s$) and deterministic model coefficient ($w_{k,i}^s$):

$$\mathcal{H}_{k,i,t}^s[I_t^s, R_t^s, \mathcal{R}_{k,i,t}^s(P_t^s, E_t^s)] = \left[\frac{k_{2_k} \cdot c_{p_{k,i,t}}^{\ s} - c_{s_{k,t}}}{k_{1_k} \cdot c_{s_{k,t}}^{\ s} - c_{0_{k,t}}^{\ s}}\right] r_{k,i,t}^s - w_{k,i}^s \qquad (3.39)$$

With this last equation, the input-output model with hydrologic variability is fully determined, including endogenous changes in the water use coefficients, due to the natural hydrologic variability calculated by the multivariate model.

The following values for the model parameters of COD concentration and runoff/recharge ratios are considered in this study.

c_{s_k}	=	20 mg/l
$c_{0_k}^{min}$	=	15 mg/l
$c_{0_k}^{max}$	=	25 mg/l
$c_{0_k}^{mean}$	=	20 mg/l
π_k^{min}	=	0.5
π_k^{max}	=	1.5
π_k^{mean}	=	1.0

3.5 Defining a scarcity threshold

3.5.1 Endogenous scarcity threshold

Sturla and Rocchi (2022) incorporate intra-annual variability, calculating the EWEI for the critical month, comparing its value with respect to the thresholds defined in the literature and based on the 100 years simulated. One of the sustainability criteria used is that for all years the EWEI in the critical month is equal to or less than 1. However, no specific threshold is defined for the EWEI at the annual resolution.

This study proposes a water scarcity threshold for the (annual) EWEI, considering the intra-annual variability of water demand and supply. This threshold is endogenous with respect to the economic and hydrological structure of each subregion *s*.

Consider α^s the proportion of extended demand corresponding to industries showing intra-annual variability and a_i^s the percentage of extended demand in month *i* with respect to the annual average (distribution factor), in subregion *s*. In addition, consider β^s the proportion of feasible surface water supply, b_i^s the intra-annual surface water distribution factor and c_i^s the intra-annual groundwater distribution factor, in subregion *s*. Thus, the EWEI on a monthly scale can be expressed as:

$$EWEI_i^s = \frac{(1-\alpha^s)\cdot\frac{ED^s}{12} + \alpha^s\cdot\frac{ED^s}{12}\cdot a_i^s}{(1-\beta^s)\cdot\frac{FS^s}{12}\cdot c_i^s + \beta^s\cdot\frac{FS^s}{12}\cdot b_i^s} \tag{3.40}$$

Where ED^s and FS^s are the extended demand and the feasible supply considering both groundwater and surface water. Using the definition of the

$EWEI^s$ (annual) from equation (3.10) we have that the monthly indicator can be written as:

$$EWEI_i^s = \frac{(1-\alpha^s) + \alpha^s a_i^s}{(1-\beta^s)c_i^s + \beta^s b_i^s} EWEI^s \tag{3.41}$$

where,

$\alpha^s = \frac{ED_{Var}^s}{ED^s}$	Proportion of extended demand corresponding to industries with intra-annual variability
$\beta^s = \frac{FS_{sw}^s}{FS^s}$	Proportion of surface water feasible supply
$a_i^s = \frac{ED_{Var,i}^s}{ED_{Var}^s/12}$	Intra-annual distribution coefficient of the extended demand corresponding to industries with intra-annual variability
$b_i^s = \frac{FS_{sw,i}^s}{FS_{sw}^s/12}$	Intra-annual distribution coefficient of surface water feasible supply
$c_i^s = \frac{FS_{gw,i}^s}{FS_{gw}^s/12}$	Intra-annual distribution coefficient of groundwater feasible supply

The scarcity threshold corresponds to the annual $EWEI^s$ that ensures that in no month the $EWEI_i^s$ will be greater than 1, for the subregion *s.* ST^s can be represented as:

$$ST^s = \min_i \frac{(1-\beta^s)c_i^s + \beta^r b_i^s}{(1-\alpha^s) + \alpha^s a_i^s} \tag{3.42}$$

This scarcity threshold is defined for the average hydrological conditions and allows comparison with the $EWEI^s$ value calculated for each simulated hydrological year.

It is important to take into account also the possibility of groundwater and surface water regulation within the year. Therefore, we introduce the concept of scarcity threshold with integrated water management. In particular, the intra-annual distribution coefficients of the feasible supply (c_i^r, b_i^r) depend on the regulation capacity of groundwater and surface water. For groundwater, it is possible to carry out an intra-annual regulation given its intrinsic nature to regulate the flow (natural impoundment). In the case of surface waters, the existence and type of regulation infrastructure (hydraulic works) will determine the degree of intra-annual regulation.

The scarcity threshold (ST_m^s) with integrated groundwater and surface water management will correspond to the value of the expression in equation (3.42) maximized by the sets of c_i^r and b_i^r values:

$$ST_m^s = \max_{c_i^s, b_i^s}\left[\min_i \frac{(1-\beta^s)c_i^s + \beta^r b_i^s}{(1-\alpha^s) + \alpha^s a_i^s}\right] \quad (3.43)$$

For groundwater, management is always possible. It is considered a range $c_i^r \in (1-\delta^s, 1+\delta^s)$, where δ^s corresponds to the percentage by which the groundwater supply in month *i* can be above or below the annual average.

A similar scheme is proposed for surface water, however, the parameters will strongly depend on the existence and type of regulation infrastructure. It is considered a range $b_i^s \in (1-\rho^s, 1+\rho^s)$, where ρ^s corresponds to the percentage by which the surface water supply in month *i* can be above or below the annual average.

For the purposes of this study, only the groundwater discharge capacity is considered, defining the scarcity threshold by considering groundwater optimal management (ST_g^s) as the following:

$$ST_g^s = \max_{c_i^s}\left[\min_i \frac{(1-\beta^s)c_i^s + \beta^r b_i^s}{(1-\alpha^s) + \alpha^s a_i^s}\right] \quad (3.44)$$

Of course, this threshold is less restrictive than the previously defined threshold (ST^s). We assume a value of $\delta^s = 30\%$ for all subregions.

3.5.2 Data for the estimations

For base hydrological conditions we consider the parameters used by Sturla and Rocchi (2022) for the intra-annual structure of agricultural extended water demand and surface water feasible supply. For climate change hydrological conditions we use the estimations of D'Oria et al. (2019) for surface water feasible supply.

For water supply, the seasonal runoff factors correspond to the average measured for the Arno River, the most important surface watercourse in Tuscany (Autorità di distretto dell'Appennino Settentrionale, 2021). Table 3-1 shows the monthly surface water supply factors.

Table 3-1. Monthly surface water supply factors

Month	$g_{R,j}$
Jan	1.655
Feb	1.788
Mar	1.579
Apr	1.349
May	0.923
Jun	0.517
Jul	0.190
Aug	0.137
Sep	0.251

Month	$g_{R,j}$
Oct	0.606
Nov	1.381
Dec	1.624

Source: Autorità di distretto dell' Appennino Settentrionale (2021)

For surface and groundwater demand from agriculture, the seasonal variation estimated by Venturi et al. (2014) is considered. Table 3-2 shows the monthly agricultural water demand factors.

Table 3-2. Monthly agricultural demand factors

Month	$g_{A,j}$
Jan	0.064
Feb	0.064
Mar	0.064
Apr	0.097
May	0.719
Jun	2.877
Jul	4.992
Aug	2.587
Sep	0.343
Oct	0.064
Nov	0.064
Dec	0.064

Source: Venturi et al. (2014).

For the climate change hydrology we considere the coefficients estimated by D'Oria et al. (2019) for the surface water intra-annual supply (Table 3-2).

Table 3-2. Monthly surface water supply factors

Month	$g_{R,j}$
Jan	1.582
Feb	1.916
Mar	1.406
Apr	1.212
May	0.778
Jun	0.382
Jul	0.203
Aug	0.146
Sep	0.269
Oct	0.650
Nov	1.714
Dec	1.741

Source: D'Oria et al. (2019)

3.6 Hydro-economic equilibrium

3.6.1 Defining hydro-economic equilibrium

Local hydro-economic equilibrium (LHEE) for subregion s is defined as the situation where the $EWEI^s$ is less than or equal to the ST_g^s considering average hydrological conditions.

Regional Hydro-Economic Equilibrium (RHEE) is defined as the situation where all LLSs satisfy the LHEE. That is, there is no water stress in any subregion s. The economic equilibrium can be written as:

$$\frac{(v_{blue}^s + v_{grey}^s)^T \cdot L^s \cdot y}{FS^s} \leq ST_g^s \quad ,\forall s \tag{3.45}$$

Where v_{blue}^s and v_{grey}^s corresponds to the *(m x 1)* vectors of blue (groundwater and surface water) and grey (water for dilution) water use intensity coefficients by industry in subregion *s*, considering average hydrological conditions (the average of the *N* simulations). The feasible supply FS^s is also considered for the average hydrological conditions. The L^s *(m x mn)* matrix corresponds to the Leontief inverse matrix blocks associated with production in the subregion s and the *(mn x 1)* vector y is the final demand.

3.6.2 Opportunity cost of the hydro-economic equilibrium

The opportunity cost of the hydro-economic equilibrium is calculated on the basis of the reduction in output required to bring all subregions into the hydro-economic equilibrium. The optimization problem to be solved has the objective function of maximizing production (minimum reduction) by varying the final demand without restrictions in deficit subregions (the final demand can be zero).

The final demand in each subregion is modified on the basis of the control variable ϕ^s. The production vector x is redefined as:

$$x = L \cdot \hat{\phi} \cdot y \tag{3.46}$$

Where $\hat{\phi}$ is a diagonal *(mn x mn)* matrix containing *m* times the value of ϕ^s for each of the *n* subregions.

We define e as the *(mn x mn)* vector of ones, T denotes the transpose and Γ is the set of subregions with deficits. The optimization problem is:

$$\max_{\phi} e^T \cdot L \cdot \hat{\phi} \cdot y$$
$$s.t.$$
$$\frac{(v_{blue}^s + v_{grey}^s)^T \cdot L^s \cdot \hat{\phi} \cdot y}{FS^s} \leq ST_g^s \leq ST^r \quad , \quad \forall r \tag{3.47}$$
$$\theta^s \in [0,1] \quad , \quad \forall r \in \Gamma$$

Consider x^* as the production vector after the optimization process and x^b as the production vector in the base situation (the current production of the economy). The opportunity cost of the hydro-economic equilibrium is (CHEE):

$$CHEE = e^T \cdot (x^* - x^b) \tag{3.48}$$

The cost of the hydro-economic equilibrium refers to the regional hydro-economic equilibrium (RHEE). When using an IRIO model, any reductions in production necessary to satisfy the local hydro-economic equilibrium (LHEE) in subregion *s* will have an impact on the other sub-regions (with and without deficit). The IRIO model developed in this study allows to know the reduction of production in each of the *n* subregions.

3.7 Coefficients of withdrawal and discharge

The coefficients used by Rocchi and Sturla (2021) are considered, adjusted based on ISTAT and IRPET. Withdrawals and discharge coefficients were estimated only for industries that directly withdraw from water bodies (*extracting* sectors). We hypothesize that water used in all other productive activities (forest, fishery, electricity transmission and distribution, steam and air conditioning supply and the whole service sector) is purchased from the water supply sector and discharged through the sewerage service sector.

3.7.1 Agriculture

The estimation of irrigation needs has been first developed at the municipal level.

The municipalities were aggregated by irrigation districts based on geographical and climatic similarities. To each climatic area, a unit irrigation need has been assigned for different groups of crops, derived from bibliographic and research data, mainly from experimental tests carried out by irrigation extension services in Tuscany.

Since most of the experimental data on irrigation needs in Tuscany relate to the Val di Chiana, Val di Cornia and Grosseto areas, the determination of the irrigation needs of the other areas has been carried out using specific conversion coefficients. The coefficients were defined by comparing the potential evapotranspiration (ETP) measured by the meteorological stations present in each irrigation district with those of the reference zones for experimental studies.

Specific assumptions have been made on irrigation needs of crops with peculiar water requirements, such as nursery productions or tobacco cultivation in the Val di Chiana and Valtiberina areas.

The estimates of irrigation requirements described above provides average theoretical irrigation intakes by municipality and by hectare of crop typology. The total withdrawals for irrigation include an additional amount of water corresponding to an average efficiency level of 70% in the use of water.

The total withdrawals have been calculated multiplying the unitary water withdrawal coefficients to the total areas cultivated for each crop typology resulting from the ARTEA database.

The withdrawals at the municipal level have been divided between underground sources (wells and springs) and surface sources of supply (reservoirs, lakes, rivers and streams) from the information available in the 2010 General Agricultural Census at the municipal level.

The estimates of water withdrawals by crop typology have been reclassified into the eight sub-sectors of Tuscan agriculture. A particular elaboration of the data of the census of Tuscan agriculture made it possible to map the withdrawals at the municipal level to the withdrawals that can be attributed to each subsector of regional agriculture. First, the water withdrawals for irrigation calculated for each municipality have been divided among farm types according to their share of Utilized Agricultural Area (UAA). Second, the total withdrawals assigned to each FT were subdivided between surface and ground water according to the share of each source of water provisioning at the municipality level resulting from the General Census of Agriculture.

Based on water withdrawals, for each subsector of agriculture in each LLS also discharge coefficients were quantified, representing the share of water returned to water bodies. The amount of water not incorporated into final products depends on losses due to inefficiency of irrigation systems (30% of total withdrawals) and natural losses of soil moisture by evaporation (discharges to the hydrological cycle). Natural losses have been quantified as a percentage of green water withdrawals, based on technical coefficients from literature. We assumed that the whole amount of discharges due to inefficiency of irrigation systems returns to ground water bodies.

The estimation of water use coefficients for livestock production activities was based on technical literature about the needs of water per head of livestock per day. Specific coefficients by species and typology of livestock unit (age, production type) were applied to the composition of the regional herd. A non-published study carried out by the National Research Council Center for Agriculture (CREA) to quantify water requirements of the Italian livestock sector at the municipality level was the source of information used to disaggregate at the sub-regional level the total regional requirements. Water requirements of each subsector were allocated between ground and surface water in the same proportion of irrigation withdrawals. The estimated total consumption was then distributed among the different FTs based on their share in the rearing of Livestock Units, according to standard results from the European Farm Accountancy Data Network (FADN) public database[3].

Based on technical literature, discharges have been quantified as a fixed proportion of withdrawals (13%) and assumed to be returned only to groundwater bodies.

3.7.2 Manufacture

Water requirements of manufacture activities have been quantified using non-published data used by ISTAT to produce the report on "Water Use and Quality in Italy", for year 2019 (https://www.istat.it/it/archivio/234904). Based on several sources of information, both from direct surveys and administrative records, ISTAT provided water withdrawals coefficients for Italian economic activities disaggregated up to four digits (235 groups) of the classification of production activities (ATECO). Sub-regional coefficients were obtained weighting the national ones according to the composition (subsectors included) of the 29 aggregated manufacture sectors represented in the IO table. Coefficients were weighted based on the value of gross output of production units, resulting from the permanent census of manufacturing and construction activities (FRAME SBS Territoriale), a geo-referenced database of all manufacturing production units. The implicit assumption is that, different from agriculture, the average water requirements of manufacture are not affected by location (as is conversely likely to be in the case of agriculture).

The share of different sources in water withdrawals and the water discharge coefficients were calculated using information from the Exiobase database. Exiobase (https://www.exiobase.eu/) is a global multi-regional system of input-output-hybrid tables, i.e., extended to environmental components. It has been developed for research purposes by harmonizing existing input-output tables for several countries, linking them with tables of trade flows between countries and adding information and estimates on emissions and resource use from different productive sectors. Ratios and shares for Italian

[3]https://agridata.ec.europa.eu/extensions/FarmEconomyFocus/FADNDatabase.html

manufacturing activities resulting from Exiobase were applied to the estimated water withdrawals by industry.

The distribution of water extraction coefficients for production activities between groundwater and surface water was based on reasonable ad hoc assumptions. In general, it was assumed that the sources of direct water supply for manufacturing activities were surface water bodies. For some industries, supply was divided between surface and groundwater based on the breakdown of sources for civilian use resulting from the 2015 ISTAT Water Census. As regard to water discharges, we assumed that, except for the Mining and Quarrying case, discharges were directed to surface water bodies. Finally, losses to the hydrological cycle, due to evaporation, were quantified as a fixed proportion of discharges to surface water bodies.

3.7.3 Water supply industry

For the purpose of calculating the withdrawal and discharge coefficients in the water supply industry, calculations are made for each municipality of Tuscany and then aggregated at LLS level (each LLS is a set of municipalities).

We following steps:

- calculation of the percentage of water losses by municipality;
- calculation of total water billed by municipality;
- estimation of total water withdrawals by municipality;
- disaggregation of withdrawals by water source and by municipality;
- aggregation of the municipality's water withdrawal and discharge volumes by LLS;
- estimation of withdrawal and discharge coefficients.

Water losses are estimated considering the water that enters the communal networks and the water actually supplied to the final users taking the year 2018 as reference (ISTAT, 2021); the difference corresponds to water losses.

The information on water billed by municipality for year 2016 was obtained from Autorità Idrica Toscana (2017). The total water withdrawals correspond to the water billed plus the losses.

To disaggregate the withdrawals between groundwater and surface water sources, regional information from ISTAT (2021) is used. The same composition is assumed for each municipality as more detailed information is not available. The water discharges correspond to the estimated losses for each municipality, and it is assumed that these are received only by groundwater bodies.

The groundwater and surface water withdrawal volumes and the volumes of water discharged to groundwater are aggregated at the LLS level. Finally, the withdrawal and discharge coefficients are estimated by dividing the volumes by the output of the water supply industry at each LLS.

3.7.4 Electricity production

For the production of electricity sector, all the existing generators in Tuscany and their annual energy production, for the year 2018, have been considered at the municipality level (GSE, 2022). We assume that the generation in reference year (2017) had the same structure.

Considering the characteristics of the generation technologies, the most appropriate water coefficients for each unit of energy produced have been used (Macknick et al., 2012; Spang et al., 2014; Bakken et al., 2013).

In this way it is possible to determine for each generation technology (wind, geothermal, hydroelectric, solar and geothermal) the following quantities by municipality:

- water withdrawals;
- water consumptions;
- water discharges.

Water consumption correspond mainly to evaporation in hydroelectric, thermoelectric and geothermal power plants, and is considered as a discharge to the natural hydrological cycle. Water withdrawals are considered to be from surface sources and discharges (non-consumption associated with the hydrological cycle) are also considered to be towards surface sources.

Withdrawals are assumed to be entirely from surface water and water discharges are assumed to be to surface water and to the hydrological cycle (evaporation).

Based on this information, water withdrawal and discharge volumes by municipality are aggregated at LLS level. Coefficients are calculated dividing the total estimated water by dividing this volumes by the output of the water supply industry at each LLS.

3.8 Water for dilution parameters

The COD concentration in the discharges are estimated based on the estimates for Tuscany carried out by Rocchi and Sturla (2021). Since the grey water calculation in this study considers the maximum COD limits defined in the discharge regulations, the same parameters are considered for each LLS.

For the total reaction rate of pollutants after entering the water bodies and the pollution purification rate before entering the water bodies, we use the values used by Guan and Hubacek (2008) and Rocchi and Sturla (2021), considering the same values for each LLS.

5 RESULTS

5.1 Extended demand and Feasible supply

Table 4-1 shows the spatial statistics considering average hydrology conditions (the mean of the 100 simulations) for the extended demand (blue and grey water), the water required for dilution (grey water), the green water demand (agriculture) and the total feasible supply. Dilution water represents 66% of the extended demand, which in turn corresponds to 24% of the feasible supply (a regional EWEI of 0.24). The demand for green water has the highest spatial variability and asymmetry with a coefficient of variation of 158% and a skewness of 2.5. Regarding the first order spatial autocorrelation, water for dilution has the highest value (0.369). Table 4-3 shows the values of this water demand components by LLS.

Table 4-1. Spatial statistics for demand and supply variables

Spatial Statistics	Extended demand (gw+sw)	Water for dilution	Green water demand	Feasible supply
Mean (Mm^3)	28.0	18.4	22.7	118.8
SD (Mm^3)	32.7	23.6	35.8	133.2
CV	117%	129%	158%	112%
Skewness	2.5	2.4	2.5	1.9
Min (Mm^3)	0.0	0.0	0.0	3.3
Max (Mm^3)	159.3	113.0	179.0	514.6
Moran Index (1^{st} ord.)	0.270	0.369	0.199	0.294

Source: own elaboration

Figure 4-1 shows the average extended demand of groundwater and surface water (blue and grey water) by LLS. Firenze and Prato are the "outliers" subregions with the highest demand in volumetric terms (Mm^3). When considering the water extended demand intensity (m^3/€), i.e. divided by the total production of each LLS, Rosignano Maritimo, Pomarance, Piombino and Orbetello are the "outliers" subregions.

Figure 4-2 presents the average grey and green water demand by LLS. The greatest demand for green water is concentrated in the southern part of Tuscany where agricultural activity is substantially higher. The grey water demand map is quite similar to the extended demand map (Figure 4-1) given the high impact of this component.

Regarding the temporal variability, Figure 4-3 shows the coefficient of variation (calculated on the basis of the 100 simulations) of the extended demand (blue and grey water) and the green water demand. The southern Tuscany area presents a higher variability of the extended demand due to the replacement of green water by blue water in agriculture and the changes generated in dilution water due to the change in COD concentration in the water sources. In the case of green water demand, the coefficient of variation is much smaller (than in the case of ED) and does not show a spatial structure associated with agricultural activity in southern Tuscany.

Figure 4-1. Average Extended demand (blue and grey water)
(Volumetric measure and intensity)

ED Volumetric (Mm^3) ED Intensity (m^3/€)

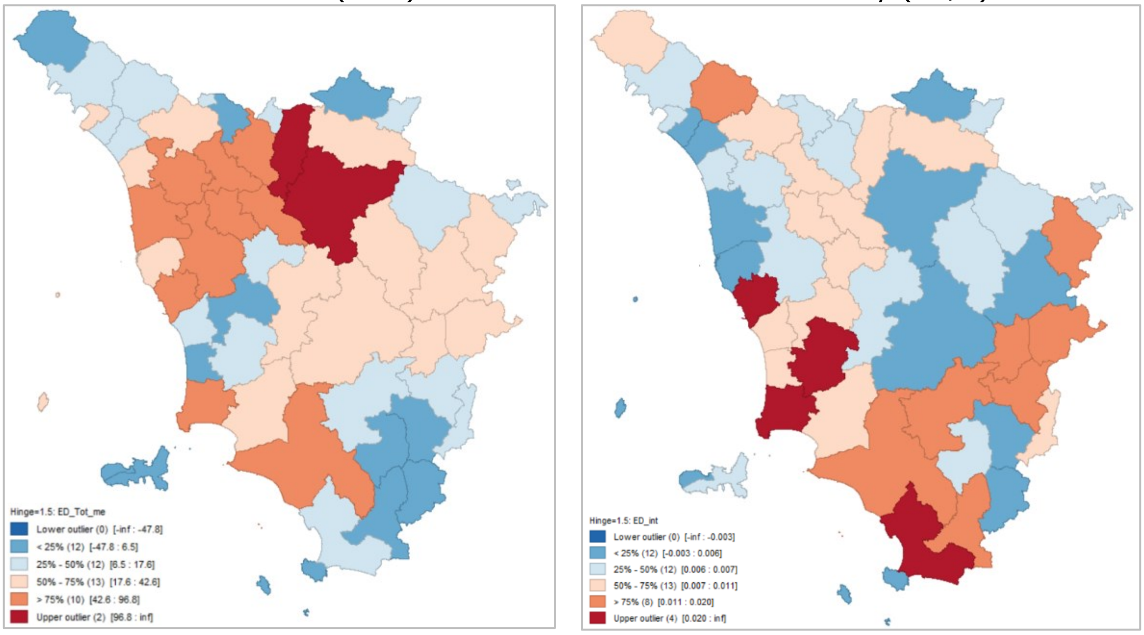

Source: own elaboration

Figure 4-2. Average Green and Grey water demand

Green water (Mm^3) Grey water (Mm^3)

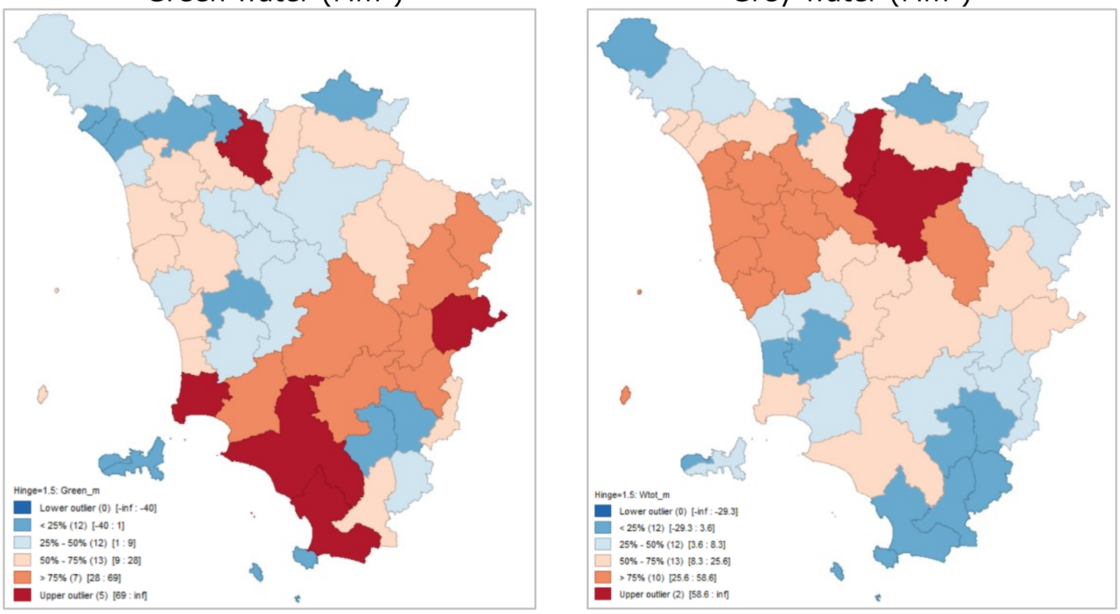

Source: own elaboration

Figure 4-3. Variation Coefficient of Extended demand and Green water demand

Extended demand | Green water demand

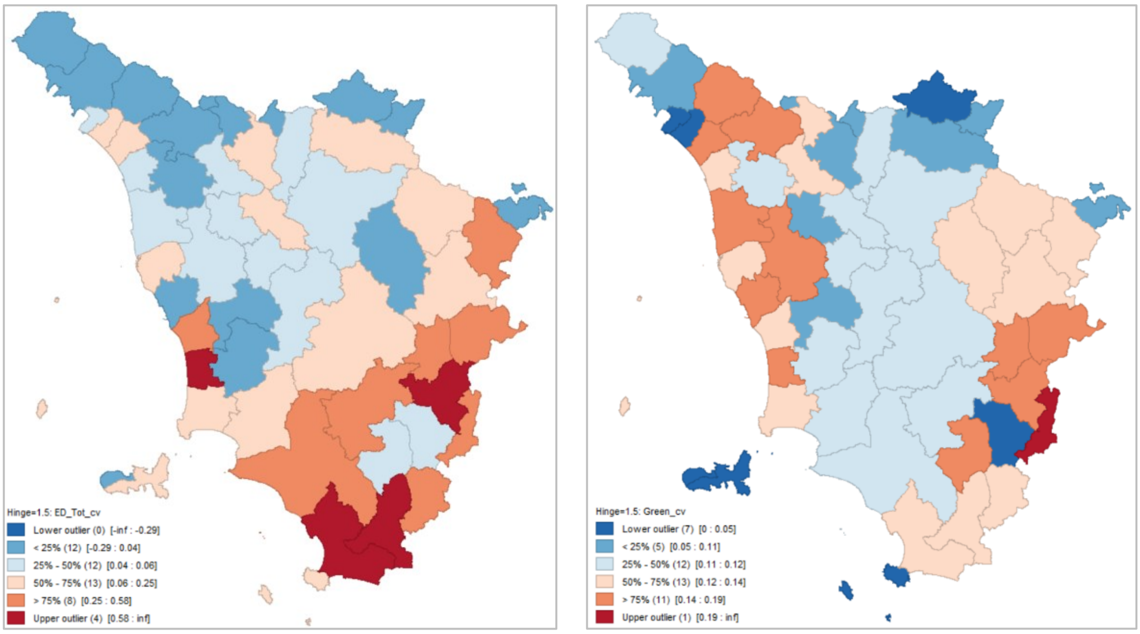

Source: own elaboration

Regarding the feasible supply, Figure 4-4 presents the average value and the coefficient of variation by LLS. A higher feasible supply can be seen in the northern area and in the upper areas of Tuscany. The coefficient of variation is high in the LLSs located in northern Tuscany and in some upper parts, for these cases the standard deviation is quite high as both the average and the coefficient of variation are high. This is mainly linked to the variability of precipitation.

Figure 4-4. Feasible supply (average and coefficient of variation)

Average FS (Mm^3) | Variation Coefficient FS

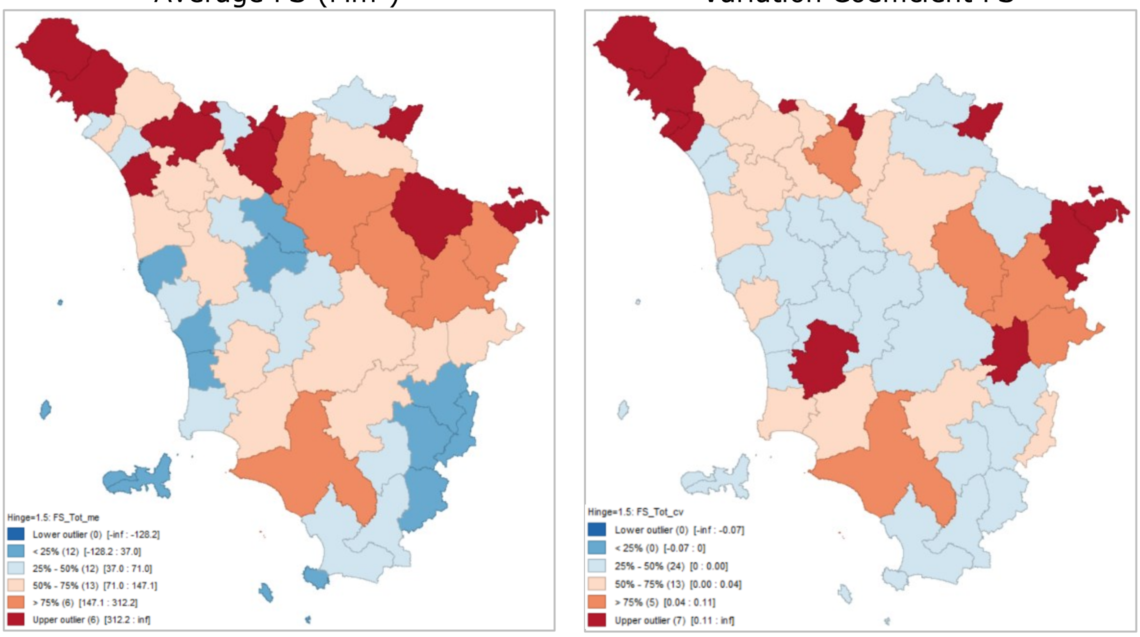

Source: own elaboration

A fundamental aspect of the feasible supply corresponds to surface water concessions, which limit the use of water. There is a high heterogeneity of the M_s parameter (ratio between concessions and surface runoff), with an average of 38.5% and a coefficient of variation of 124%. This parameter conditions the spatial structure of the feasible supply, which differs from the natural availability.

Figure 4-5 presents the spatial heterogeneity of the M_s parameter and Table 4-2 shows it spatial frequency analysis. For 19 of 49 LLS less than 9 % of the surface runoff is conceived and in 13 LLS over 50 %.

Figure 4-5. Surface water Concessions
(% of surface runoff)

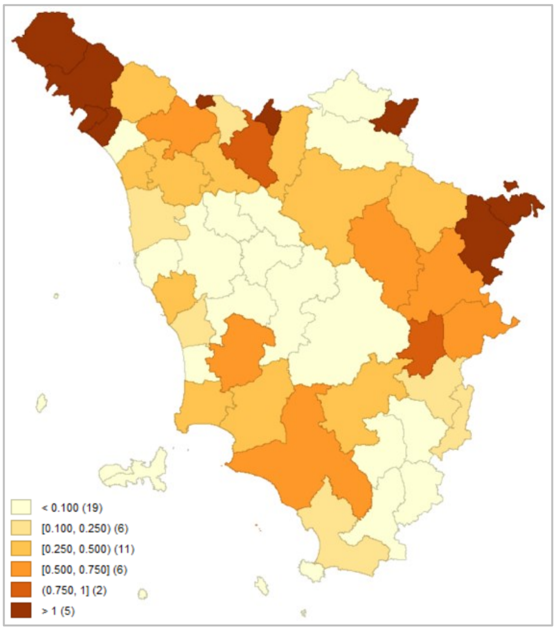

Source: own elaboration

Table 4-2. Concessions Ms

% of Runoff	Number of LLS
0-9%	19
10-24%	6
25-49%	11
50-74%	6
75-99%	2
>100%	5

Source: own elaboration

Table 4-3. Average results by LLS

SLL	Extended demand (gw+sw) (Mm^3)	Water for dilution (Mm^3)	Green water (Mm^3)	Feasible supply(Mm^3)	EWEI	STg	EWEI>STg
CARRARA	19.2	14.8	0.0	57.6	0.36	0.61	0
MASSA	16.4	13.7	0.0	141.0	0.13	0.34	0
PONTREMOLI	4.2	2.8	1.0	380.1	0.01	0.33	0
BARGA	19.4	10.3	0.1	514.6	0.04	1.00	0
CASTELNUOVO DI	11.2	5.9	0.8	147.1	0.08	0.92	0

SLL	Extended demand (gw+sw) (Mm^3)	Water for dilution (Mm^3)	Green water (Mm^3)	Feasible supply(Mm^3)	EWEI	STg	EWEI>STg
GARFAGNANA							
LUCCA	70.2	47.1	11.7	120.6	0.59	0.95	0
PIETRASANTA	9.6	8.3	0.1	45.9	0.21	1.00	0
VIAREGGIO	35.0	28.2	7.5	355.0	0.10	1.00	0
MONTECATINI-TERME	56.2	38.0	27.9	71.0	0.80	0.73	58
PISTOIA	43.7	25.6	78.0	466.2	0.10	0.47	0
SAN MARCELLO PISTOIESE	1.7	0.5	0.0	37.0	0.05	1.00	0
BORGO SAN LORENZO	18.3	11.5	15.7	78.4	0.24	0.72	0
CASTELFIORENTINO	10.8	8.6	3.0	26.7	0.41	1.00	0
EMPOLI	53.3	47.0	2.1	35.1	1.54	1.00	100
FIRENZE	159.3	113.0	1.8	149.6	1.07	0.97	96
FIRENZUOLA	0.3	0.1	0.0	43.3	0.01	0.63	0
CASTAGNETO CARDUCCI	3.4	0.7	14.1	16.2	0.23	0.28	27
CECINA	10.0	5.4	20.5	33.8	0.31	0.44	16
LIVORNO	42.6	43.0	9.2	30.6	1.41	1.00	100
MARCIANA MARINA	0.0	0.0	0.0	3.3	0.00	1.00	0
PIOMBINO	64.9	18.6	126.0	47.2	1.42	0.39	100
PORTOFERRAIO	6.1	6.2	0.0	15.1	0.41	1.00	0
ROSIGNANO MARITTIMO	50.1	29.8	6.7	37.2	1.36	0.85	100
PISA	46.0	34.3	17.5	72.6	0.64	0.84	1
POMARANCE	12.4	1.3	1.2	91.1	0.14	0.68	0
PONTEDERA	44.8	50.1	12.6	75.2	0.60	0.99	0
SAN MINIATO	55.2	47.3	2.0	39.1	1.43	1.00	100
VOLTERRA	5.4	3.6	0.4	39.0	0.14	1.00	0
AREZZO	36.5	21.7	65.4	183.2	0.21	0.38	3
BIBBIENA	10.5	6.5	13.7	428.5	0.03	0.59	0
CORTONA	23.6	10.0	72.8	94.9	0.28	0.24	36
MONTEVARCHI	39.9	26.7	9.1	160.1	0.26	0.67	0
SANSEPOLCRO	17.9	6.3	63.2	209.3	0.10	0.21	8
CHIUSI	6.5	4.0	15.5	18.7	0.37	0.31	44
MONTALCINO	11.3	3.8	43.4	80.0	0.15	0.24	12
MONTEPULCIANO	14.8	5.2	55.5	37.0	0.42	0.25	50
PIANCASTAGNAIO	3.3	1.9	0.0	36.2	0.09	1.00	0
POGGIBONSI	28.3	20.6	0.6	64.1	0.45	1.00	0
SIENA	37.0	24.9	35.6	135.1	0.28	0.69	0
SINALUNGA	17.6	7.8	47.2	75.8	0.26	0.27	35
CASTEL DEL PIANO	2.9	2.0	0.1	39.3	0.07	1.00	0
FOLLONICA	17.6	7.6	31.5	85.1	0.21	0.38	3
GROSSETO	56.7	25.5	179.0	201.6	0.29	0.25	48
MANCIANO	4.4	0.8	20.4	39.4	0.12	0.25	13
MONTE ARGENTARIO	0.8	1.3	0.0	5.2	0.15	1.00	0
ORBETELLO	16.7	2.8	77.7	68.7	0.26	0.22	41
PITIGLIANO	0.7	0.1	1.9	28.9	0.03	0.35	0
PRATO	147.5	100.7	18.0	163.2	0.91	1.00	19
EXTRA_TOS	8.5	5.7	1.2	495.3	0.02	0.47	0

Source: own elaboration

5.2 EWEI and Scarcity threshold

Table 4-4 shows the spatial statistics considering average hydrology conditions (the mean of the 100 simulations) for the extended water exploitation index (*EWEI*), the scarcity threshold with optimal intra-annual management of groundwaters (*STg*), and the times with which *EWEI* is greater than *STg* (frequency in 100 years). The *EWEI* presents more variability and asymmetry than the *STg*, but *STg* is a variable with more spatial autocorrelation. Table 4-3 shows the values of this water demand components by LLS.

Table 4-4. Spatial statistics for *EWEI* and *STg*

Spatial Statistics	EWEI	STg	EWEI>STg
Mean	0.38	0.67	20.61
SD	0.43	0.31	33.68
CV	111%	46%	163%
Skewness	1.6	-0.2	1.6
Min	0.00	0.21	0
Max	1.54	1.00	100
Moran Index (1st ord.)	0.338	0.396	0.155

Source: own elaboration

Figure 4-6 shows the average and the coefficient of variation of the *EWEI*. It can be seen that there are 12 LLS for which the *EWEI* is higher than 0.42 and for 5 of them it is higher than 0.9 (central Tuscany area). For the LLS located in the southern part of Tuscany, the *EWEI* presents a higher variability, due mainly to the variability of the Extended demand.

Figure 4-6. Average and variation coefficient of EWEI indicator

Average EWEI (Mm^3) Variation Coefficient EWEI

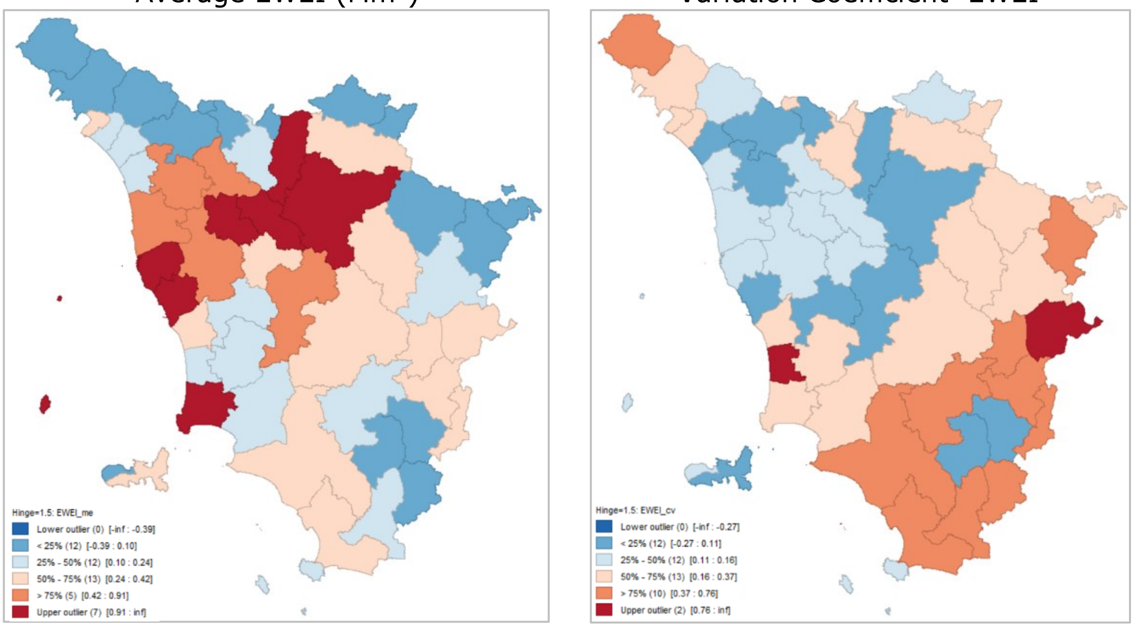

Source: own elaboration

Figure 4-7 presents a map with the *STg* and the times with which the *EWEI* is greater than the *STg* (frequency in 100 years). The value of *STg* depends on the relative percentage of agriculture and feasible surface water supply in each LLS. Given the heterogeneity of the *Ms* parameter (concessions), there is a dominance of the effect of surface runoff on agriculture, which is reflected in a higher value of *STg* in central and northern Tuscany. It can be seen that for 27 LLS the EWEI never exceeds the scarcity threshold, and for 14 LLS it is exceeded more than 25 times, with 5 LLS where it is always exceeded (Table 4-5). Figure 4-8 presents a graph both the scarcity threshold without optimal management of groundwaters (*ST*) and with optimal management (*STg*), can be seen that while *STg* is always greater than *ST*, the effect is greater for some LLS.

Figure 4-7. Scarcity Threshold and Frequency with which EWEI is greater than STg

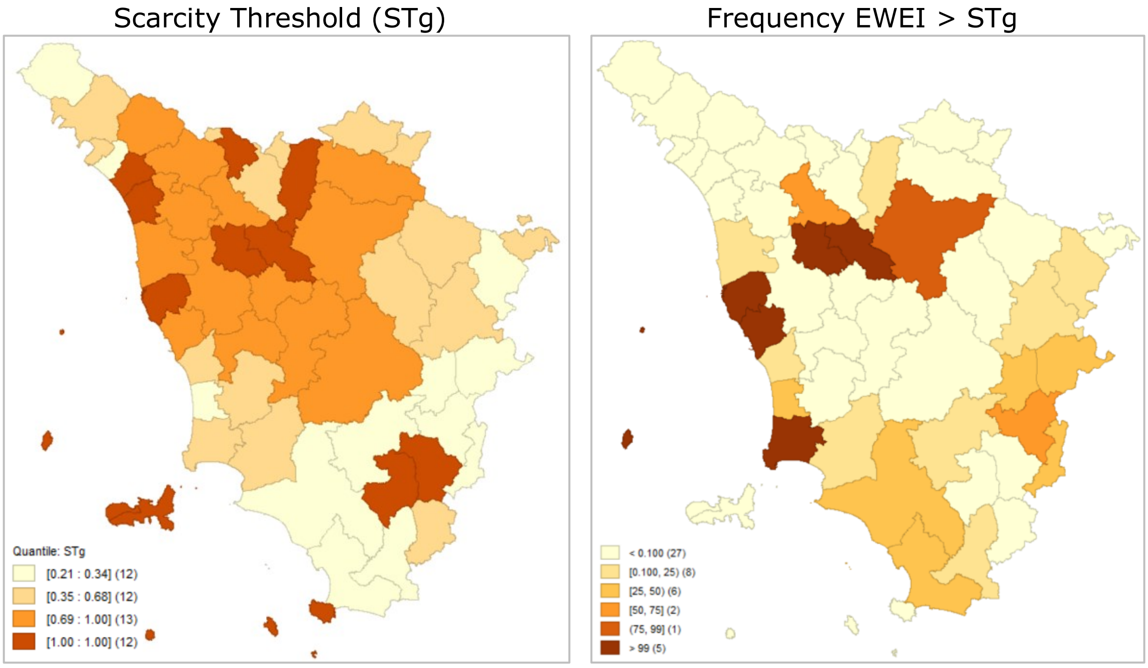

Source: own elaboration

Table 4-5. Frequency EWEI greater than STg

Frequency in 100 years	Number of LLS
0	27
1-24	8
25-49	6
50-74	2
75-99	1
100	5

Source: own elaboration

Figure 4-8. Average EWEI, ST and STg by LLS

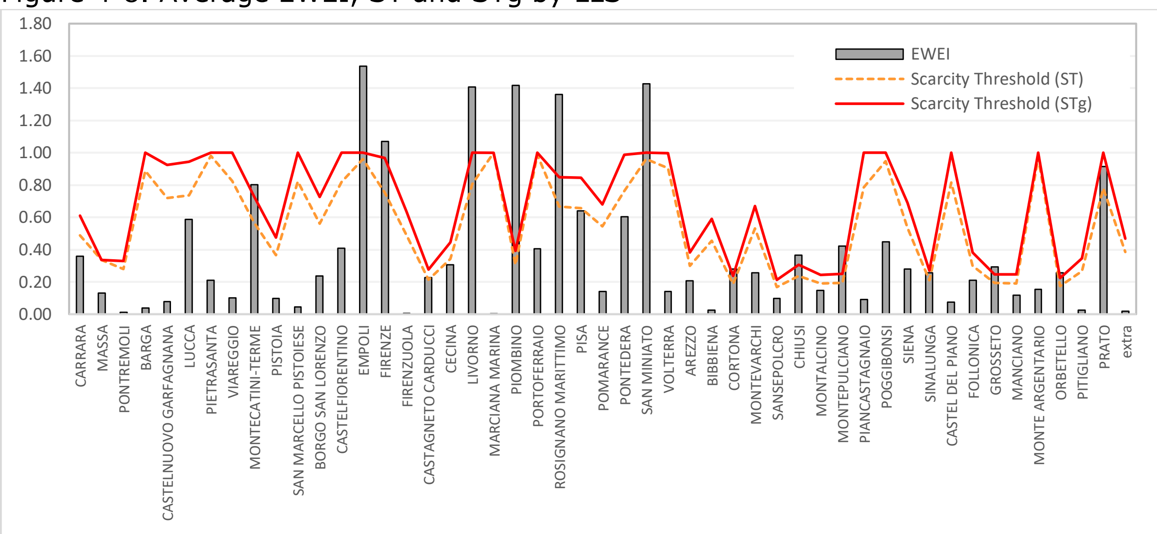

Source: own elaboration

5.3 Hydro-economic equilibrium

For the average hydrology conditions there are 12 LLS that not satisfy the local hydro-economic equilibrium (LHEE), i.e., where the average *EWEI* is greater than the Scarcity Threshold. Figure 4-9 presents a map with this 12 LLS and Table 4-6 shows the respective values por the average *EWEI*, the *STg* and the frequency with which *EWEI* is greater than STg.

Figure 4-9 Average hydro-economic equilibrium

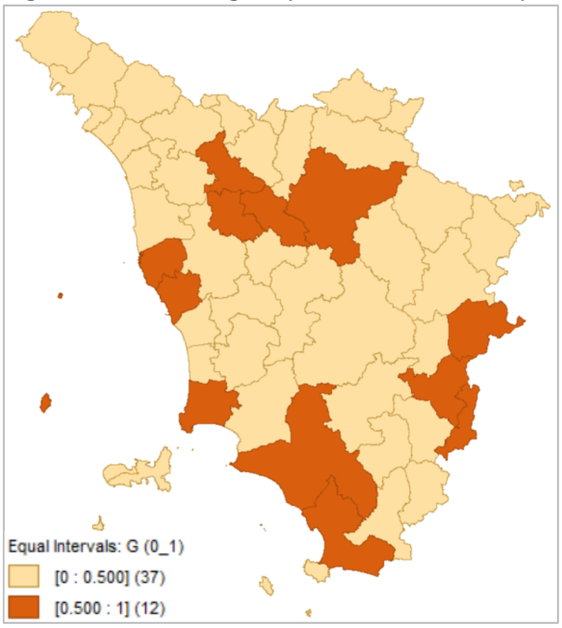

Source: own elaboration

Table 4-6. LLS that not satisfy the hydro-economic equilibrium

SLL	EWEI	STg	Frequency EWEI > STg
MONTECATINI-TERME	0.80	0.73	58
EMPOLI	1.54	1.00	100
FIRENZE	1.07	0.97	96
LIVORNO	1.41	1.00	100
PIOMBINO	1.42	0.39	100
ROSIGNANO MARITTIMO	1.36	0.85	100
SAN MINIATO	1.43	1.00	100
CORTONA	0.28	0.24	36
CHIUSI	0.37	0.31	44
MONTEPULCIANO	0.42	0.25	50
GROSSETO	0.29	0.25	48
ORBETELLO	0.26	0.22	41

Source: own elaboration

Regional hydro-economic equilibrium (RHEE) corresponds to the situation where all LLS satisfy the LHEE. The opportunity cost of the hydro-economic equilibrium has been defined in this study as the optimal reduction of the production by varying the final demand in the LLSs with problems. The estimated opportunity cost of the hydro-economic equilibrium is 21,298 million of Euro corresponding to the 9.94% of the total production in Tuscany.

Since the IRIO model is used in the linear optimisation problem, the output necessarily falls in all LLS. Figure 4-10 presents a map with the output reduction. It can be seen that for 43 LLS the reduction of production is greater than 2%, for 11 LLS it is greater than 5%, for 8 LLS it is greater than 10% and for 6 of them it is greater than 25% (Table 4-7).

Figure 4-10. Opportunity Cost of the Hydro-economic Equilibrium.
(Percentage of production reduction)

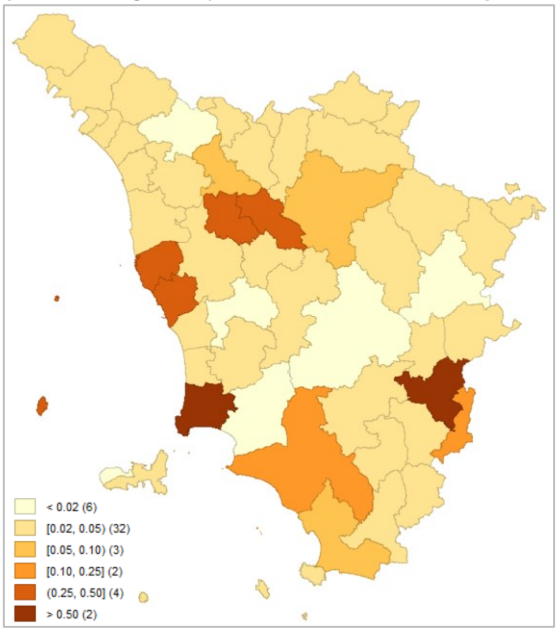

Source: own elaboration

Table 4-7. Percentage of production reduction

Reduction of Production	Number of LLS
<2%	6
2-5%	32
5-9%	3
10-24%	2
25-49%	4
>50%	2

Source: own elaboration

5.4 Climate Change

Considering the hydrology with climate change the EWEI presents an increase in all LLS, however with heterogeneous spatial effects. Figure 4-11 shows the EWEI recalculated for a climate change scenario and also (right side) a comparison percentage with the base scenario. A greater effect is seen in southern Tuscany mainly due to the higher presence of agriculture, a sector that has to replace green water more intensively with blue water. For 10 LLS the change is greater than 20% and for 2 LLS it is greater than 25% (Table 4-8).

Figure 4-11. Average EWEI climate change scenario
(Climate change and CC vs Base scenario)

Climate change (Average EWEI) | CC vs Base (%)

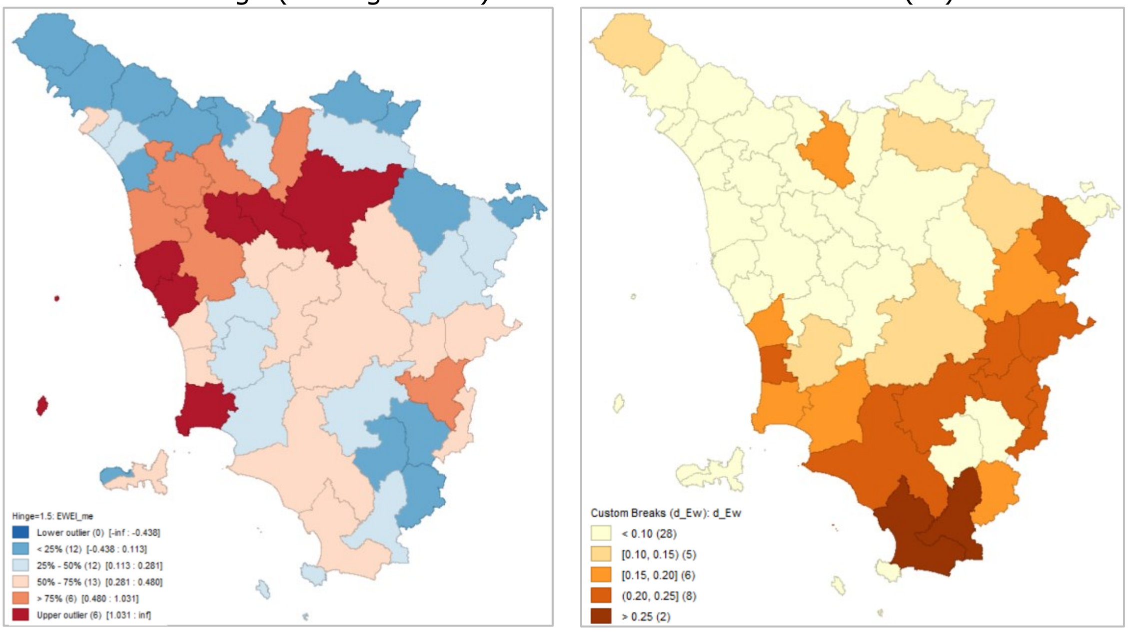

Source: own elaboration

Table 4-8. Increase in EWEI with climate change

EWEI increase	Number of LLS
0-9%	28
10-14%	5
15-19%	6
20-25%	8
>25%	2

Source: own elaboration

In the case of the scarcity threshold, while the average across LLSs decreases slightly from 0.672 to 0.665 (1%), it is noticeable that for some LLSs it decreases and for others it increases. For 7 LLS the reduction is more than 5% and for 1 LLS the increase is more than 5% (Figure 4-12, Table 4-9). The decrease is associated with a higher share of demand from the agricultural sector in the total and/or a higher share of feasible surface water supply in the total feasible supply. The opposite is true for the increase in STg, which partly compensates for the increase in EWEI in the 13 LLS where this occurs.

Figure 4-12. Scarcity threshold (STg) climate change scenario
(Climate change and CC vs Base scenario)

Climate change | CC vs Base scenario (%)

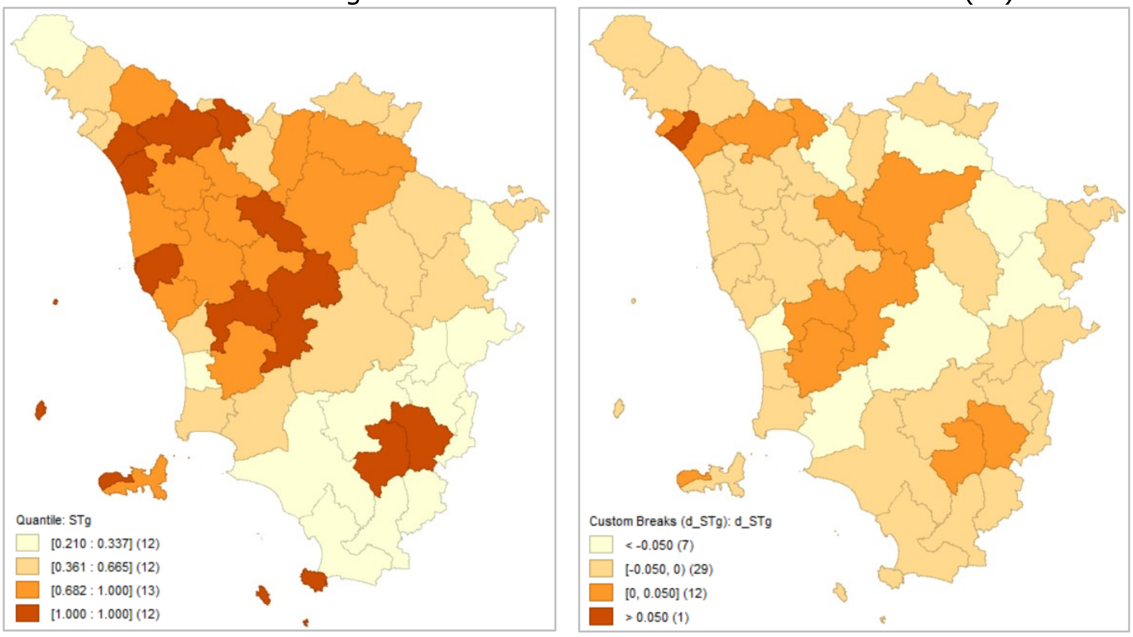

Source: own elaboration

Table 4-9. Change in STg for climate change
(CC vs Base scenario)

Change STg	Number of LLS
<-5%	7
-5 to 0%	29
0 to 5%	12
>5%	1

Source: own elaboration

Regarding the frequency (in 100 years) with which the EWEI exceeds the scarcity threshold, an increase is observed for 18 LLS. For 8 LLS the increase is greater than 10 years and for 2 LLS greater than 20 years. Figure 4-13 and Table 4-10 show this results.

Figure 4-13. Frequency EWEI greater than STg climate change scenario (Climate change and CC vs Base scenario)

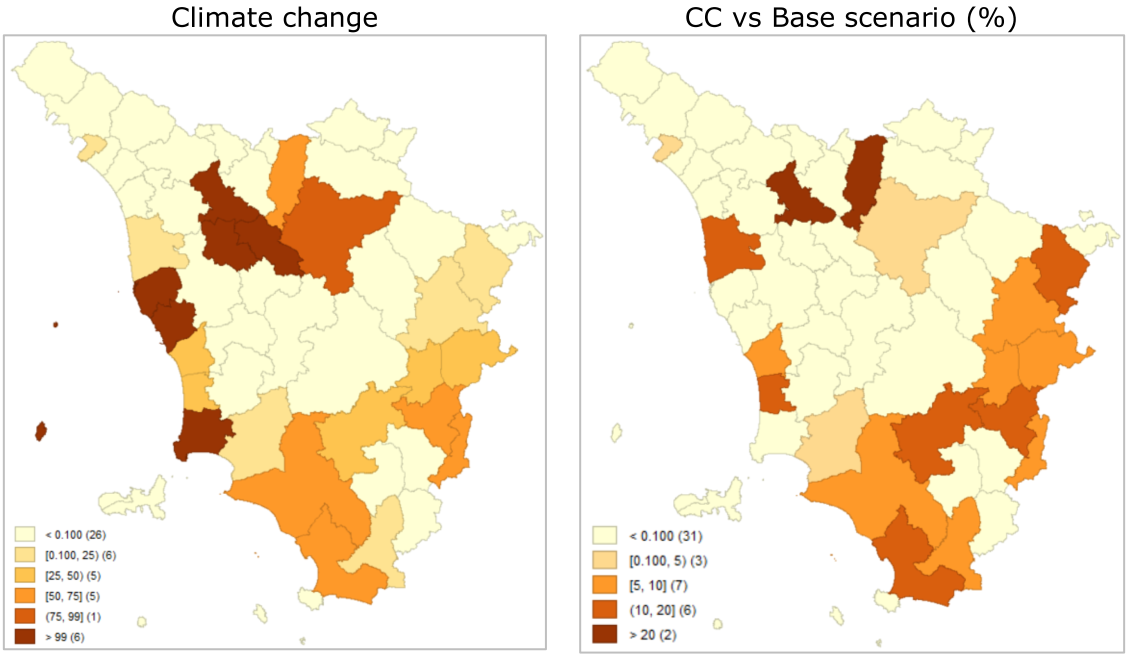

Source: own elaboration

Table 4-10. Frequency EWEI greater than STg (Climate change vs Base scenario)

Frequency	Number of LLS
0	31
1-4	3
5-10	7
11-20	6
>20	2

Source: own elaboration

For the scenario with climate change in 14 LLS there is no hydro-economic equilibrium for the average hydrological conditions. Two LLS are added with respect to the baseline scenario: Castagneto Carducci and Sinalunga (Figure 4-14).

Regarding the opportunity cost of the hydro-economic balance, with climate change this corresponds to 30,035 million euros (14% of total production), 8,737 million euros more than in the baseline scenario. For 11 LLS the percentage increase in production reduction compared to the baseline scenario is more than 2.5% (Figure 4-15). Table 4-11 presents a comparison between the two scenarios, where it can be seen that for the case with climate change all LLS have a production reduction of more than 2% (43 in the base case) and for 10 LLS the production reduction is more than 25% (6 in the base case).

Figure 4-14. Average HEE climate change scenario

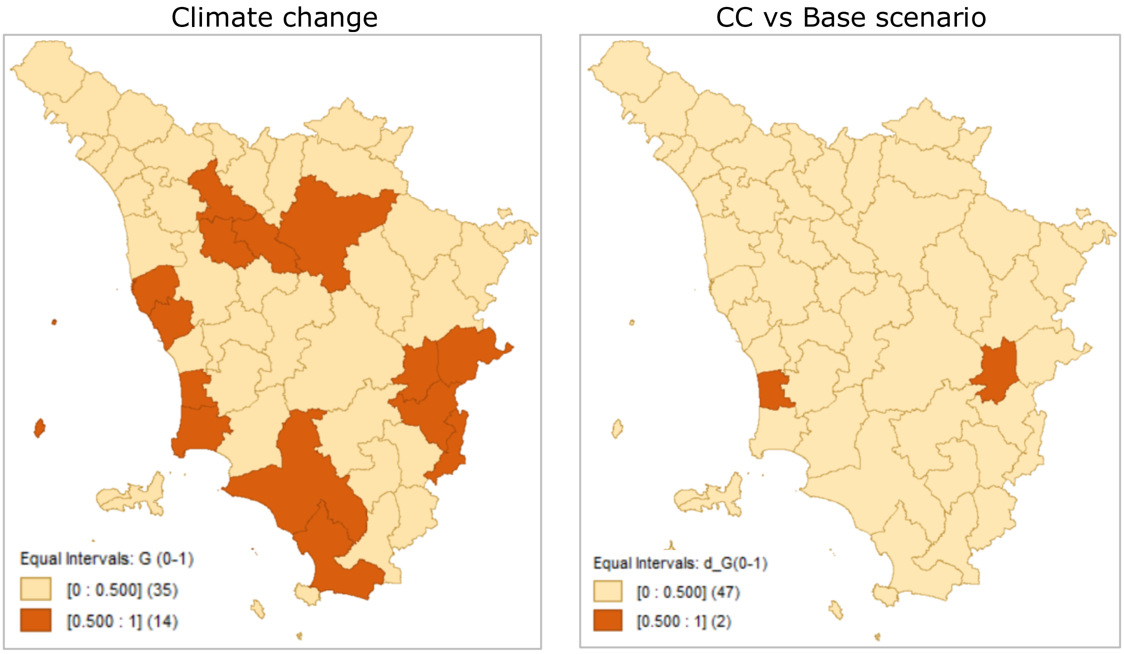

Source: own elaboration

Figure 4-15. Opportunity Cost of the HEE. Percentage of production reduction (Climate change and CC vs Base scenario)

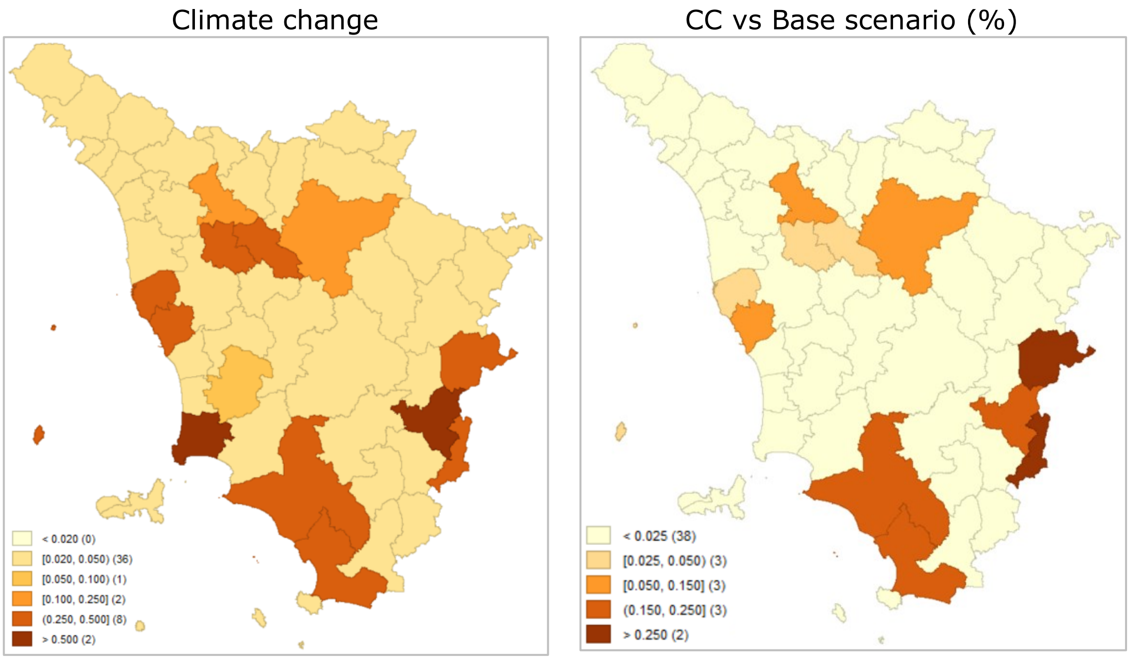

Source: own elaboration

Table 4-11. Percentage of production reduction
(Climate change vs Base scenario)

Reduction of Prod.	N° of LLS Base scenario	N° of LLS Climate change
<2%	6	0
2-5%	32	36
5-9%	3	1
10-24%	2	2
25-49%	4	8
>50%	2	2

Source: own elaboration

5.5 Aggregated regional results

In the study developed by Sturla and Rocchi (2022) results were obtained for the *EWEI* at regional level considering hydrological variability (100 years). The results of the hydro-economical model IRIO have been aggregated at regional level to obtain the *EWEI* of Tuscany. The Scarcity Threshold (*STg*) has been calculated for both cases. Figure 4-16 shows the comparison of the results. Although for none of the simulated hydrological years the regional scarcity threshold is exceeded, the cumulative probability distribution present a different shape in both models, which is explained by aggregation biases. Two of the most important biases correspond to: i) the large heterogeneity in the distribution of surface water allocations, and ii) the variability of precipitation that conditions the replacement of green water by blue water and the water required for dilution (grey water). As can be seen in Figure 4-16 the average EWEI is higher in the case of the aggregated subregional model (0.24 vs. 0.21). The variance is 8% greater in the aggregated IRIO model and the skewness is lower the aggregated IRIO model (0.64 vs. 1.25). The STg in the IRIO aggregated model is 0.590 and in the regional model is 0.576.

Figure 4-16. EWEI comparison between IO and IRIO hydro-economic Model

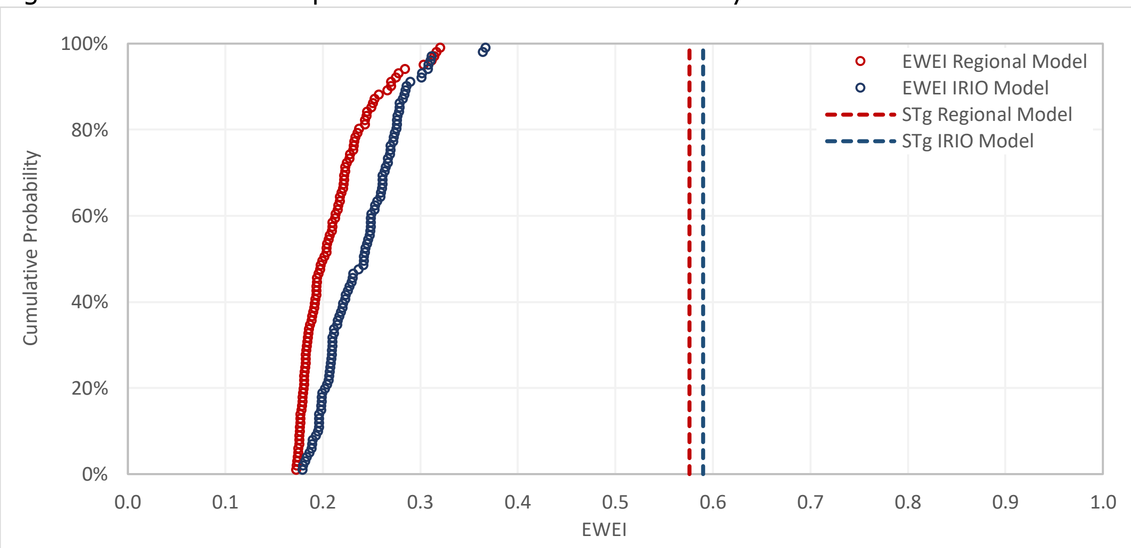

Source: own elaboration

Figure 4-17 presents the comparison between the aggregation of the IRIO hydro-economic model results considering the base hydrology and the climate change hydrology. For the case with climate change, the EWEI increases from 0.24 to 0.27, the variance increases by 24% and the skewness increases by 24%. Although for the case with climate change the maximum EWEI increases (0.45) it is still below the scarcity threshold (0.562). However, the situation changes dramatically when considering spatial disaggregation, as discussed in the previous sections.

Figure 4-17. EWEI comparison between IRIO results for base and climate change hydrological conditions

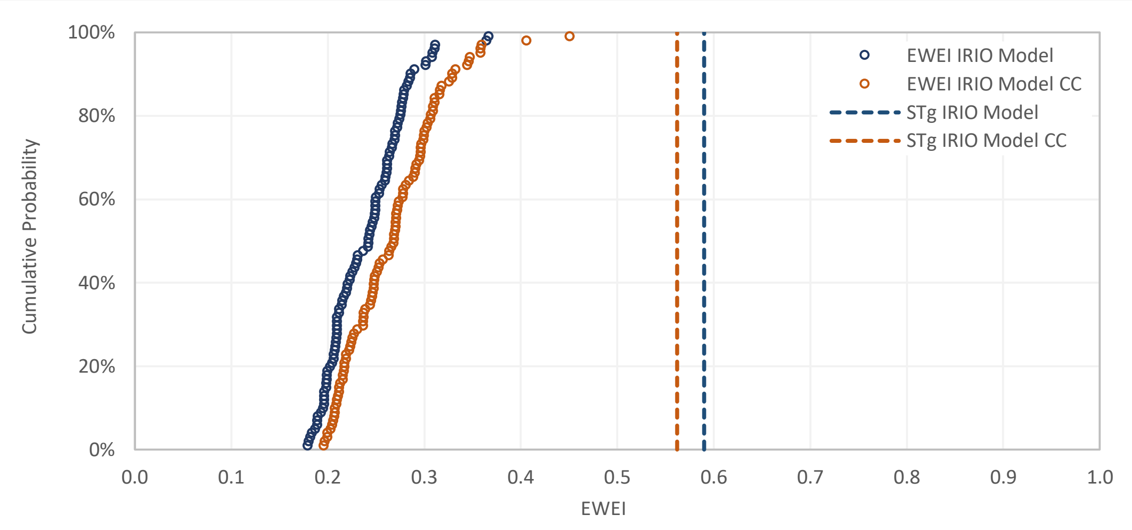

Source: own elaboration

7 DISCUSSION AND CONCLUSIONS

In this paper we study the relationship between economy and water resources in Tuscany through a hydro-economic, multi-regional input-output model. The model provides an accurate representation of the regional economy, subdivided into 49 Local Labour Systems, groups of contiguous municipalities classified according to an economic criterion (minimizing the flows of commuters who the boundaries across LLSs), and 53 industries. Production activities withdraw from and discharge water towards three different water bodies (groundwater, surface water and the hydrological cycle), according with industry-specific water coefficients. The extended water demand is defined as withdrawals (blue and green water) minus discharges plus the water requirements for dilution (grey water). We measure the intensity of pressures exterted by the economic system on water resoureces through an Extended Water Exploitation Index (EWEI), the ratio of extended water demand to a "feasible" measure of water supply, taking into account natural as well as technological and institutional (e.g. water concession) constraints to water availability.

The model includes the hydrological variability of water supply, calibrated to replicate the observed data at the subregional level. An endogenous variability of demand is included as well, generated by the adaptation of the demand to natural variability of green water supply in agriculture (substitution of green water with blue water with irrigation) and to the dependence of grey water demand on the natural variation of runoff in surface water bodies. The inclusion of the hydrological variability allows to consider the EWEI as a random variable and to study its cumulative distribution function using Montecarlo techniques, under different climatic scenarios. The model allows to assess the water balance and the extent of pressures on water resources at different geographical scales: from single LLSs to the whole region.

We first use the model to study the hydroeconomic equilibrium defining a water scarcity threshold (ST) for the annual EWEI, given the intra-annual variability of water demand and supply. The scarcity threshold corresponds to the annual EWEI ensuring that in no month the EWEI is greater than 1, i.e. that the extended demand is never higher than the feasible supply. The concept of ST is applied also at the regional level as the average *regional* EWEI ensuring that the *local* ST are never trespassed in all subregional units. Interestingly, due to the variability of the hydrological balance, the ST is variable as well and endogenously determined by the economic and hydrological structure of each subregion. Our results show that both with the average hydrology and under a scenario with climate change, the regional EWEI never trespasses the regional scarcity threshold. This apparent "sustainable" use of water in Tuscany hides a relevant spatial variability, showing an unsustainable use of water (EWEI > ST) at the sub-regional level, namely for 12 over 49 LLS with average hydrology and 18 over 49 under the climate change scenario. Beside this first relevant result, the multi-scale nature of the model allows us to quantify the bias of

aggregation in the determination of the regional EWEI and ST, that are underestimated when quantified using an aggregate regional model.
We then calculated the opportunity cost of the regional hydro-economic balance as the minimum reduction in the gross output of the regional economic system compatible with a sustainable use of water in all LLS. According to our results, under the average hydrology the hydroeconomic balance would require a descrease of the regional gross output equal to 21,298 million of Euro corresponding to the 9.94% of the total production in Tuscany. The estimated cost increses to 30,035 million euros (14% of total production) under the climate change scenario.
The model is suitable to several applications both to support water management at the regional level and to get further methodological advances. The concept of hydro-economic equilibrium and the quantification of its opportunity cost could be used in the economic assessment of public investment programmes to improve the sustainability of the regional hydro-economic system both on the supply side (works for the regulation of surface water) and on the demand side (improving the efficiency in the use of water for irrigation). Moreover, the model could be used to support the design of regional policy for the management of water resources, such as the definition of additional quality constraints in the discharge of water used in production activity as well as the spatial optimization of concession for blue water withdrawals.
As regard as to methodological advances, a first natural development of this study is the analysis of the bias in using standard rules for the scarcity-weighted measures of water footprint. As our results clearly show, the thresholds of the average aggregated measures identifying scarcity problems in water use strictly depends on the temporal and spatial variability of the hydro-economic balance. An equal aggregated value of a given exploitation index of water resource in two countries, could reflect completely different levels of stress on water resources, depending on the specific structure of their hydroeconomic systems (spatial and temporal variability). Moreover, different spatial scales of the analysis could imply different biases in the measurement of water scarcity, depending on the criteria used to define the spatial units of analysis (economic vs. hydrological).
Finally, a further development of the analysis could be associating the physical balance of water resources with a monetary estimation of the flows of ecosystem services generated by the hydrological system. A promising tool to support the representation of the ecosystem service flows in the model is the new System of Environmental-Economic Accounting for Ecosystem Accounting (United Nations et al., 2021) recently released by UN and other international bodies.

9 REFERENCES

1. Alcamo, J., Henrich, T. and Rosch, T. (2000). "World Water in 2025—Global Modelling and Scenario Analysis for the World Commission on Water for the 21st Century". *Centre for Environmental System Research*. Report A0002. University of Kassel: Kassel, Germany.
2. Autorità di distretto dell'Appennino Settentrionale. (2021). "Piano di gestione delle acque". https://www.appenninosettentrionale.it/itc/
3. Autorità Idrica Toscana (2017) "Consumi idrici per gestore e commune, 2016". https://www.autoritaidrica.toscana.it/
4. Bakken, T.H., Killingtveit, Å., Engeland, K. and Harby, A. (2013). "Water consumption from hydropower plants – review of published estimates and an assessment of the concept" *Hydrology and Earth System Science*. 17, 3983–4000, 2013.
5. Bartolini, G., Messeri, A., Grifoni, D., Mannini, D. and Orlandi, S. (2014). "Recent trends in seasonal and annual precipitation indices in Tuscany (Italy)". *Theoretical and Applied Climatology.* 118:147‑157. DOI 10.1007/s00704-013-1053-3
6. Bartolini, G., Grifoni, D., Mano, R., Torrigiani, T. and Gozzini, B. (2018). "Changes in temporal distribution of Precipitation in a Mediterranean area (Tuscany, Italy) 1955–2013". *International Journal of Climatology.* V. 38, pp. 1366-1374.
7. Braca, G., Bussettini, M., Lastoria, B., Mariani, S., and Piva, F. (2021)." Il Bilancio Idrologico Gis BAsed a scala Nazionale su Griglia regolare – BIGBANG: metodologia e stime". Rapporto sulla disponibilità naturale della risorsa idrica. *Istituto Superiore per la Protezione e la Ricerca Ambientale*. Rapporti 339/21, Roma.
8. Braca, G., Bussettini, M., Lastoria, B., Mariani, S., and Piva, F. (2022). "Il modello di bilancio idrologico nazionale BIGBANG: sviluppo e applicazioni operative. La disponibilità della risorsa idrica naturale in Italia dal 1951 al 2020". The BIGBANG National Water Balance Model: Development and Operational Applications. *The Availability of Renewable Freshwater Resources in Italy from 1951 to 2020*. L'Acqua, 2/2022.
9. Bras, L. and Rodríguez-Iturbe, I. (1993). "Random Functions and Hydrology*". Dover, 0-486-67626-9.*
10. Brunetti, M., Maugeri, M., Monti, F. and Nanni, T. (2006). "Temperature and precipitation variability in Italy in the last two centuries from homogenised instrumental time series". *International Journal of Climatology.* 26: 345–381. DOI: 10.1002/joc.1251
11. CIRCABC (2012). "Informal Meeting of Water and Marine Directors of the European Union. Candidate and EFTA Countries". Available online: https://circabc.europa.eu/sd/a/981c1845-a59e-4f94-8770-fc5cd0626fee/Final%20synthesis%20Heraklion%20Water%20Marine%20Directors%20clean.pdf
12. Deng, G., Ma, Y. and Li, X. "Regional water footprint evaluation and trend analysis of China-based on interregional input-output model". *Journal of Cleaner Production*. 112, 4674-4682.
13. D'Oria, M., Ferraresi, M. and Tanda, M. (2019). "Quantifying the impacts of climate change on water resources in northern Tuscany, Italy, using high‑resolution regional projections". *Hydrological Processes*. 33:978–993. DOI: 10.1002/hyp.13378
14. Duarte, T. and Yang, H. (2011). Input–output and water: Introduction to the Special Issue. *Economic Systems Research*. 23:4, 341-351.

15. European Environment Agency. "The European Environment—State and Outlook 2005". European Environmental Agency: Copenaghen, Denmark, 2005.
16. European Environment Agency (2020). "Use of freshwater resources in Europe". Available online: https://www.eea.europa.eu/data-andmaps/indicators/use-of-freshwater-resources-3/assessment-4
17. Faergemann, H. (2012). "Update on Water Scarcity and Droughts indicator development. In EC Expert Group on Water Scarcity & Droughts". *European Environment Agency*. Brussels, Belgium; pp. 1–23.
18. Fatichi, S. and Caporali, E. (2009). "A comprehensive analysis of changes in precipitation regime in Tuscany*". International Journal of Climatology*. V. 29, pp. 1883-1893.
19. Garcia-Hernandez, J. and Brouwer, R. (2021). "A multiregional input–output optimization model to assess impacts of water supply disruptions under climate change on the Great Lakes economy". *Economic Systems Research*. 2021, Vol. 33, No. 4, 509–535. https://doi.org/10.1080/09535314.2020.1805414
20. GSE (2022). "Elenco impianti elettrici". *Gestore Servizi Elettrici, Italia.*
21. www.gse.it
22. Guan, D. and Hubacek, K. (2008). "A New and Integrated Hydro-Economic Accounting and Analytical Framework for Water Resources: A Case Study for North China". *Journal of Environmental Management. 88, 1300–1313.*
23. Hamilton, J.D. (1994). "Time Series Analysis". *Princeton University Press*. 1st Edition.
24. Hoekstra, A.Y., Chapagain, A.K., Mekonnen, M.M. and Aldaya, M.M. (2011). "The Water Footprint Assessment Manual: Setting the Global Standard". *1st ed.; Earthscan: London, UK.* ISBN 978-1-84977-552-6.
25. ISTAT (2010). "General Agricultural Census at the municipal level". *Istituto Nazionale di Statistica.* Italia. http://censimentoagricoltura.istat.it/
26. ISTAT (2019). "Water Use and Quality in Italy". *Istituto Nazionale di Statistica.* Italia. https://www.istat.it/it/archivio/234904
27. IRPET (2021). "Interregional Input-Output Table for the Tuscany Region, Italy". *Istituto Regionale di Programmazione Económica Regione Toscana.*
28. Isard, W., et al. (1960). "Methods of Regional Analysis: An Introduction to Regional Science". *MIT Press*.
29. ISTAT (2021). "Banchi di dati e sistemi informazioni". https://www.istat.it/it/dati-analisi-e-prodotti/banche-dati
30. Lenzen, M.,Moran, D., Bhaduri, A., Kanemoto, K., Bekchanov, M., Geschke, A., and Foran, B. (2013). "International trade of scarce water. *Ecological Economics"*. *94*, 78–85. https://doi.org/10.1016/j.ecolecon.2013.06.018
31. Macknick, J., Newmark, R., Heath, G and Hallett, K.C. (2012). "Operational water consumption and withdrawal factors for electricity generating technologies: a review of existing literature". *Environmental Resource Letters.* 7, 045802 (10pp).
32. Maity, R. (2018). "Statistical Methods in Hydrology and Hydroclimatology". *Springer Transactions in Civil and Environmental Engineering.*
33. Meng, Yu., Chunhui, Li., Xuan, W., Yanpeng, C., and Wencong, Y. (2017). "Optimal water utilization and allocation in industrial sectors based on water Footprint accounting in Dalian City, China". *Journal of Cleaner Production*. 1-9.
34. Miller, T., and Blair, P. (2009). "Input-Output Analysis: Foundations and Extensions". *Cambridge University Press*. 2nd Edition.

35. OECD. (2015). "Water: Freshwater abstractions (Edition 2015)". OECD Environment Statistics (database). https://doi.org/10.1787/f9f5fcd1-en
36. Pacetti, T., Castelli, G., Schröder, B., Bresci, E. and Caporali, E. (2021). "Water Ecosystem Services Footprint in Agricultural Production in Central Italy". Science of the Total Environment. 797, 149095.
37. Pfister, S., Koehler, A. and Hellweg, S. *(2009).* "Assessing the Environmental Impacts of Freshwater Consumption in LCA*". Environ. Sci. Technol. 43, 11, 4098–4104. https://doi.org/10.1021/es802423e*
38. Pranzine, G., Di Martino, F., Della Santa, E., Fontanelli, K. and Fucci, G. (2020). "Impact of climate change on the water balance of the Apuo-Versilia plain aquifer (Tuscany, Italy)". *Italian Journal of Groundwater.* DOI 10.7343/as-2020-474
39. Raskin, P., Gleick, P.H., Kirshen, P., Pontius, R.G. and Strzepek, K. (1997). "Comprehensive Assessment of the Freshwater Resources of the World" *Document prepared for UN Commission for Sustainable Development 5th Session*. Stockholm Environmental Institute: Stockholm, Sweden.
40. Rencher, A. and Christensen, W. (2012). "Methods of Multivariate Analysis". *Wiley-Interscience*.
41. Rocchi, B. and Sturla, G., (2021). "An input-output hydro-economic model to assess the economic pressure on water resources in Tuscany". *Working Papers-Economics*. WP18/2021. DISEI. University of Florence.
42. Rossi, G. and Caporali, E. (2010). "Regional Analysis of low flow in Tuscany (Italy)". *Global Change: Facing Risk and Threats to Water Resources*. IAHS Publ. 340.
43. SIR (2021). "Strati GIS". https://www.sir.toscana.it/strati-gis
44. Spang, E.S., Moomaw, W.R., Gallagher, K.S., Kirshen, P.H., Marks, D.H. (2014). "The water consumption of energy production: an international comparison". *Environmental Resource Letters.* 9, 105002 (14pp).
45. Sturla, G. and Rocchi, B. (2022). "Incorporating hydrological variability into a hydro-economic input-output model. An application to Tuscany". *Working Papers-Economics*. WP24/2022. DISEI. University of Florence.
46. Te Chow, V. (2010). "Applied Hydrology". *Tata McGraw-Hill Education.*
47. United Nations et al. (2021). "System of Environmental-Economic Accounting—Ecosystem Accounting (SEEA EA)". White cover publication, pre-edited text subject to official editing. Available at: https://seea.un.org/ecosystem-accounting.
48. Venturi, C., Campo, L., Caparrini, F. and Castelli, F. (2014). "The assessment of the water consumption at regional scale: An application in Tuscany, Central Italy". *European Water*. V.46/46, pp. 3-23.
49. Von Storch, Hans and Francis W. Zwiers (1999). "*Statistical Analysis in Climate Research*". *Cambridge University Press.*
50. Wang, D., Hubacek, K., Shan, Y., Gerbens-Leenes, W., and Liu, J. (2021). A Review of water stress and Water Footprint Accounting". *Water*. 13, 201, pp. 1-15.
51. Wang, D., Sahu, R., Kahil, T., Tang, T. and Hubacek, K. (2022). "A Novel Integrated Hydro-Economic Model: Application to Water Stress Assessment and Mitigation in China". *Groningen University*. https://pure.iiasa.ac.at/id/eprint/18361/1/A%20Novel%20Integrated%20Hydro-Economic%20Model%20Application%20to%20Water.pdf
52. Xie, Y. (1996). "Environment and Water Quality Model". *China Science and Technology Press*, Beijing, China.

53. Zhuoying, Z., Hong, Y. and Minjun, S. (2011). "Analyses of water footprint of Beijing in an interregional input–output framework". *Ecological Economics*. 70, 2494-2502.